

The inner regions of protoplanetary disks

C. P. DULLEMOND

Max-Planck-Institute for Astronomy, Königstuhl 17, D-69117 Heidelberg,
Germany

J. D. MONNIER

University of Michigan, Astronomy Department, Ann Arbor, MI 48109 USA

Key Words planet formation, accretion, dust, infrared, radiative transfer

Abstract To understand how planetary systems form in the dusty disks around pre-main-sequence stars a detailed knowledge of the structure and evolution of these disks is required. While this is reasonably well understood for the regions of the disk beyond about 1 AU, the structure of these disks inward of 1 AU remains a puzzle. This is partly because it is very difficult to spatially resolve these regions with current telescopes. But it is also because the physics of this region, where the disk becomes so hot that the dust starts to evaporate, is poorly understood. With infrared interferometry it has become possible in recent years to directly spatially resolve the inner AU of protoplanetary disks, albeit in a somewhat limited way. These observations have partly confirmed current models of these regions, but also posed new questions and puzzles. Moreover, it has turned out that the numerical modeling of these regions is extremely challenging. In this review we give a rough overview of the history and recent developments in this exciting field of astrophysics.

CONTENTS

Introduction	2
Searching for the origin of the “near-infrared bump”	3
<i>The “near-infrared bump” and its first interpretations</i>	3
<i>Near-infrared interferometry: spatially resolving the inner disk regions</i>	6
<i>Size-Luminosity Diagram</i>	7
<i>Beyond size-luminosity relations: Inner disk shapes</i>	8
Models of the inner dust rim	10
<i>Early “vertical wall” models of the dust inner rim</i>	10
<i>Temperature of individual dust grains in the dust rim</i>	13
<i>An approximate 1-D radiative transfer model of the dust rim</i>	14
<i>Is the rim a sharp, well-defined evaporation front?</i>	15
<i>Better treatment of dust evaporation: a rounding-off of the rim</i>	16
<i>Two-dimensional radiative transfer models</i>	17
<i>To shadow or not to shadow? The debate on “puffed up inner rims”</i>	19
<i>Can the dust rim explain the NIR bump?</i>	20
<i>Behind the wall: a dust chemical reactor</i>	21
Gas inward of the dust rim	22

<i>Gas opacities</i>	22
<i>Structure of the dust-free gas inner disk</i>	23
Probing the inner dust-free disk with gas line observations	25
<i>The search for molecules in the inner dust-free disk</i>	25
<i>Probing the dynamics of the inner gas disk</i>	27
Summary and outlook	27

1 Introduction

The dust- and gas-rich disks surrounding many pre-main sequence stars are of great interest for gaining a better understanding of how planetary systems, like our own, are formed. Since the first direct Hubble Space Telescope images of such objects in silhouette against the background light in the Orion Nebula (McCaughrean & O’Dell, 1996), the observational and theoretical study of these planetary birthplaces has experienced an enormous thrust, leading to a much better understanding of what they are, what they look like, how they evolve, how they are formed and how they are eventually dissipated. While none of these aspects has yet been firmly understood in detail, there is a consensus on the big picture. It is clear that protoplanetary disks are the remnants of the star formation process. Excess angular momentum of the original parent cloud has to be shed before most matter can assemble into a “tiny” object such as a star. Protostellar accretion disks (see e.g., Hartmann, 2009, for a review) are the most natural medium by which this angular momentum can be extracted from the infalling material. When the star is mostly “finished” and makes its way toward the main sequence, the remainder of this protostellar accretion disk is what constitutes a protoplanetary disk: the cradle of a future planetary system.

Protoplanetary disks have a rich structure, with very different physics playing a role in different regions of the disk. A pictographic representation is shown in Fig. 1. One can see the strikingly large dynamic range that is involved: the outer radius of a protoplanetary disk can be anywhere from a few tens of AU up to a 1000 AU or more, while the inner disk radius is typically just a few stellar radii, i.e. of the order of 0.02 AU. This spans a factor of $10^4 \cdots 10^5$ in spatial scale. For each orbit of the outer disk we have up to ten million orbits of the inner edge of the disk. Equivalently, the dynamic time scale on which various processes in the disk take place is also a million times shorter (i.e. faster) in the very inner disk regions than in the outer disk regions. And the temperatures differ also vastly: from $T \gg 10^3$ K in the inner disk regions down to $T \sim 10 \cdots 30$ K in the outer regions.

This large dynamic range in spatial scale, density and temperature means that very different observational techniques have to be applied to probe the various regions of these disks. Long wavelength telescopes (in the far infrared and millimeter regime) predominantly probe the outer ~ 10 - few 100 AU of disks, while mid-infrared observations probe intermediate radii \sim few AU, near-infrared observations probe the inner AU and finally optical and UV observations typically probe the regions very close to the stellar surface (~ 0.01 - 0.1 AU). Of course, due to dust scattering and sometimes due to quantum-heated grains, short wavelength radiation can also be used to probe the outer disk regions, but for thermally emitted radiation from the disk this rule of thumb applies very well.

In this review we will limit our attention to the inner disk regions, roughly inward of 1 AU. This is the region of the disk where temperatures become high enough to modify, and even evaporate the dust of the disk. It is also the region where a large amount of energy is set free in the form of UV, optical and near infrared radiation, which plays a crucial role in the overall energy balance of the disk. Emission from this region is thus easily observed. But until not long ago this region of the disk had been inaccessible to spatially resolved observations because at typical distances of 100 parsec they represent structures of 10 milli-arcsecond scale, which is clearly far smaller than what today's optical and infrared telescopes can possibly resolve. Spectroscopic observations have given many hints of complex structure and interesting physics in these inner disk regions. With spatially unresolved data alone there remains, however, a lot of ambiguity in the physical interpretations of the observations.

With the advent of infrared interferometry this is now changing. It has become possible to directly spatially resolve these inner regions and verify whether the conclusions drawn from spatially unresolved spectroscopic observations in fact hold. The purpose of this review is to give an overview of the current understanding of these inner disk regions, how this understanding came about, and what are the many remaining open questions. We will mainly focus on the transition region between the dusty outer disk and the dust-free inner disk, the so called “dust inner rim” region, because it is at these spatial scales that infrared interferometry has made the largest impact. The topics of magnetospheric accretion (e.g. Bouvier et al., 2007) and jet launching (e.g. Shang, Li & Hirano, 2007), while extremely important in their own right, will be considered as separate topics and will not be covered in this review.

We will start our story with a rough historic review of how the conspicuous near-infrared bump seen in the spectral energy distributions of many protoplanetary disks led to the study of the dust-evaporation front in the disk. Then we will discuss the advances in modeling this dust-gas transition in the disk. We will subsequently discuss the physics of the dust-free inner disk, inward of the dust inner rim, and then discuss what is observed from these very inner regions in terms of gas line emission. Finally we will give a subjective outlook of remaining open issues and possible new areas of investigation.

2 Searching for the origin of the “near-infrared bump”

2.1 The “near-infrared bump” and its first interpretations

While the existence of circumstellar disks around high mass stars is still very much debated as of this writing (Cesaroni et al., 2007), the presence of such disks around young low mass pre-main sequence stars (T Tauri stars and Brown Dwarfs) and their intermediate mass counterparts (Herbig Ae/Be stars) has by now been firmly established (Watson et al., 2007). However, not all low/intermediate mass pre-main sequence stars have disks. An often used indicator of the presence of a circumstellar disk, or at least of circumstellar material, is infrared flux in excess of what can possibly be explained by a stellar photosphere of a reasonable size. By studying the fraction of stars with near infrared (NIR) excess flux in young clusters of ages from 0.5 to 5 million years, Haisch, Lada & Lada (2001) could establish a clear trend: that the “disk fraction” decreases with age, or in other words, that disks have a life time of a few million years.

A question is, however, whether one can be sure that the NIR excess is indeed from a disk and not from some circumstellar envelope or disk wind. While we know from imaging that the cold outer circumstellar material is indeed disk-like, little is known about the nature of the material inward of what telescopes can spatially resolve. The lack of correlation between A_V and NIR excess (Cohen & Kuhi, 1979) is inconsistent with a spherical dust geometry and the spectral shape of the infrared excess for T Tauri stars and Brown Dwarfs can be explained fairly well with models of irradiated dusty disks with a flat (Adams & Shu, 1986) or flared shape (Kenyon & Hartmann 1987; Calvet et al. 1992; Chiang & Goldreich 1997; Menshchikov & Henning 1997; D’Alessio et al. 1998). However, for Herbig Ae/Be stars this was initially not so clear, and still remains under debate. It appears that the JHKL photometric points nicely line up to form a “bump” very similar, though not identical, to the peak of the Planck function at a temperature of about ~ 1500 K. This is perhaps most clearly seen in the spectrum of the prototype Herbig Ae star AB Aurigae (Fig. 2). This NIR bump was not at all expected from any of the above mentioned models: They tend to yield relatively smooth “multi-color blackbody curves” in which a continuous series of Planck peaks at different temperatures add up to a smooth curve. Now there appeared to be a single Planck peak in the spectrum, albeit often with a bit of excess emission toward longer wavelengths. This “NIR bump”, as it is often called, is not just a small feature: it contains a large amount of energy. The bump alone can contain up to half the infrared flux from the entire system, and nearly all the emission originating from the inner AU or so. It can therefore not be ignored: it must be understood in terms of some physical model.

Hillenbrand et al. (1992) studied the NIR excesses of Herbig Ae/Be stars in a systematic fashion. They interpreted this bump as originating from the hot emission from an accretion disk. But to fit the NIR bump they had to make a large inner hole in the disk, with a radius of about 0.1 AU (for AB Aur, $\sim 50L_\odot$), inward of which there is no emission at all. And they had to assume a relatively large accretion rate ($\dot{M} \sim 10^{-5}M_\odot/\text{yr}$) to match the flux levels of the NIR bump. Since in standard accretion disk theory the hottest Planck component originates close to the inner radius of the disk, this means that this inner radius was set such that the temperature close to this inner radius was about 1500 K, the temperature of the NIR bump. While this fits the NIR bump, a new question emerges: If the inner edge of the accretion disk lies at ~ 5 -15 stellar radii distance from the star, where does the accreting matter go after it passes inward through this inner edge? If it would somehow continue inward, then the inevitable release of accretional energy in these inner regions would have to create hotter radiation in addition to the 1500 K emission, for the reason of energy conservation. It would thus destroy the bump-like shape of the NIR flux by filling in emission at shorter wavelength (Hartmann, Kenyon & Calvet, 1993). Alternatively, if a magnetospheric accretion scenario were responsible for this inner hole, the UV emission created by the material flowing along these field lines and crashing onto the stellar surface should be very strong, $L_{\text{accr,magn}} \simeq 2GM_*\dot{M}/R_*$. No such strong UV flux, consistent with accretion rates of the order of $\dot{M} \sim 10^{-5}M_\odot/\text{yr}$, is observed. The only alternative is that matter is simply ejected from this inner disk edge, but it is unclear how this happens, and why this inner hole is at 1500 K in nearly all sources, not at different temperatures from source to source. The Hillenbrand et al. study therefore rules out that the bump originates from

accretion alone.

So why would the NIR bump always be around 1500 K? To those who are familiar with dust physics this number immediately calls to mind the process of dust sublimation, often called “dust evaporation” in the astrophysical community. This possible association was already pointed out in the previously mentioned Hillenbrand et al. (1992) paper. Most species of interstellar dust can survive as a solid only up to about that temperature, with some rarer dust species surviving perhaps up to 1800 K. So it is a reasonable idea to propose that the NIR emitting region around Herbig Ae/Be stars consists of dust that is on the brink of evaporation. Since any model of protoplanetary accretion disks predicts that the temperature of the disk increases toward the star, it is quite reasonable to assume that inward of some radius the disk is so hot that the dust simply evaporates. Since dust is by several orders of magnitude the dominant carrier of continuum opacity of any dust-gas mixture at “low” temperatures ($< 10^4\text{K}$), the evaporation of dust in the very inner disk regions would render these disk regions much less optically thick than the dusty parts of the disk, perhaps even entirely optically thin. This means that the “dust inner rim”, the radial position separating the dusty outer regions from the dust-free inner regions, should look like a kind of optically thick “wall” of dust at the dust evaporation temperature. Inward of this wall the gas is either optically thin, or at least much optically thinner than the dust, so that this evaporation wall can be viewed by an observer right through the transparent gas in front of it, as shown pictographically in Fig. 3.

This scenario was first proposed by Natta et al. (2001, henceforth N01), in their paper on the reinterpretation of Herbig Ae/Be spectral energy distributions, and independently by Tuthill, Monnier & Danchi (2001), see Section 2.2. N01 clearly showed, using the disk model of Chiang & Goldreich (1997, henceforth C97), that a disk model that does not have such a dust evaporation wall can never fit the shape of the NIR bump, but that such an inner dust wall naturally seems to explain it. It was argued that this wall is “puffed-up” because it is much hotter than the disk behind it, and thus is likely to have a much larger vertical scale height. In a paper directly inspired by this work, Dullemond, Dominik & Natta (2001, henceforth DDN01) subsequently integrated this puffed-up inner dust rim model into the CG97 model and thus obtained a complete description of the spectral energy distributions (SEDs) of Herbig Ae/Be stars in terms of a simple irradiated disk model.

So if this simple model of the NIR bump is basically correct, then one may wonder why mainly Herbig Ae/Be stars show such a huge bump while T Tauri stars are not known for displaying such a conspicuous feature. DDN01 argue that because the stellar luminosity is at much longer wavelengths for T Tauri stars, a bump of this kind would be partly “swamped” by the flux from the star, though a close look at the spectrum should still reveal such a bump. On first sight T Tauri star SEDs do not show such a strong bump. But through a careful subtraction of the stellar spectrum, Muzerolle et al. (2003) show that also T Tauri stars consistently have such a NIR bump, though perhaps weaker in relative sense than the Herbig stars. So in that sense T Tauri stars are no different from Herbig stars.

In spite of the early success of these models, there was no easy way of telling with just NIR photometric data whether it was indeed the true nature of these objects. Indeed, much simpler spherically symmetric envelope models in which the dust was also removed inward of the dust evaporation radius, could also fit

the NIR bump and even in a number of cases the entire spectral energy distribution (Pezzuto, Strafella & Lorenzetti, 1997; Malfait, Bogaert & Waelkens, 1998; Miroshnichenko et al., 1999; Bouwman et al., 2000; Vinković et al., 2006). In fact, such models appear to be more consistent with the lack of clear observed correlation between the NIR flux and the disk inclination. For a simple perfectly vertical wall model of the rim such a correlation is clearly expected, with little NIR flux observed at near-face-on inclinations as illustrated in the left two panels of Fig. 4, and discussed in more detail in Section 3.1. Perhaps the most clear counter-example is AB Aurigae, which has a huge NIR bump (see Fig. 2), but is known to be not very far from face-on (e.g. Eisner et al., 2003; Corder, Eisner & Sargent, 2005). Note, however, that AB Aurigae is an object that is still surrounded by a substantial amount of non-disk-related circumstellar material, which may contribute to the NIR flux.

However, the key to distinguishing these models from each other is to spatially resolve the NIR disk emission. Since the spatial scale we are talking about here is about 1 AU in diameter, which means 7 milliarcseconds at typical distances of Herbig Ae stars, no NIR telescope is even remotely able to make spatially resolved images of these structures to tell which model is correct.

2.2 Near-infrared interferometry: spatially resolving the inner disk regions

Fortunately, at around the same time, a new observational technique started to become mature: the technique of infrared interferometry. This technique allows to connect two or more infrared telescopes that are tens or hundreds of meters apart, and thus achieve a spatial resolving power that far exceeds that of a single telescope. The angular scale that can thus be probed equals λ/b radians, where λ is the wavelength at which we are observing and b is the projected baseline, i.e. the distance between the telescopes as projected on the sky toward the object we observe. If we observe at $2 \mu\text{m}$ with a projected baseline of 100 meter we arrive at 2×10^{-8} radian, which is about 4 milliarcsecond. If our object is at 140 parsec this leads to a spatial resolution of about 0.6 AU, which just about matches what is needed to probe the dust evaporation front. So far, however, the complexity of infrared interferometry has restricted the number of telescopes that can participate in a single interferometric observation to just two (a single baseline) or three (three baselines). This means that, in contrast to interferometry at radio wavelengths, infrared interferometry does not yield actual aperture-synthesized images¹. It is limited to measuring “sizes”, some information about radial brightness profiles and “asymmetries” of emitting regions in the plane of the sky (see Fig. 5). Yet, as we will see, this limited information is enough to reveal a lot about the structure of the inner regions of protoplanetary disks.

The star FU Orionis was the first young star to be targeted by infrared interferometry (using the Palomar Testbed Interferometer (PTI), Malbet et al., 1998). It is the name-giving member of the class of “FU Orionis stars”, a rare class of young stellar objects with extremely high accretion rates ($\dot{M} \sim 10^{-4} M_{\odot}/\text{yr}$; Hartmann & Kenyon, 1985), which are thus very bright in the NIR. It was found that the measured “size” of the NIR emitting region of this disk matched the expectations of classical accretion disk theory. This confirms the standard concept

¹Imaging of stellar surfaces has been successful (e.g Monnier et al., 2007) with NIR interferometry just recently, but young star disks have been too faint for these techniques to date

of FU Orionis stars as being T Tauri stars with outbursting circumstellar disks.

Most T Tauri and Herbig Ae/Be stars, however, have much less active disks, and it is with those stars that infrared interferometry allowed an interesting discovery to be made. Using the Infrared Optical Telescope Array (IOTA) interferometer, Millan-Gabet et al. (1999) found that the size of the NIR emitting region for the “normal” Herbig Ae star AB Aurigae is many times larger than expected from the disk models current at that time. A similar result was found for a T Tauri star by (Akeson et al., 2000), and further work confirmed these early conclusions (especially the survey of Herbig Ae disks by Millan-Gabet, Schloerb & Traub, 2001). At that time, before the theoretical advances of the hot inner dust rim, the large measured sizes were seen to support the spherical envelopes models (e.g., Miroshnichenko et al., 1999) which had the feature of a large, optically-thin inner cavity. Also, detailed measurements of AB Aurigae showed little size variation with position angle, consistent with a spherical geometry.

On the other hand, for two bright Herbig Be stars direct evidence for disk-like (i.e. non-spherical) geometry was obtained using a variant of infrared interferometry called “aperture masking”. The aperture masking technique uses a single telescope, in this case the Keck telescope (Tuthill et al., 2000), and puts a mask in the optical beam to allow light from only a partial set of sub-apertures to interfere at the camera focal plane. This masking mimics a set of small telescopes observing simultaneously as a miniature interferometer. Since the aperture mask can contain relatively many sub-apertures, this technique allows for a true image reconstruction, in contrast to “long baseline” infrared interferometry. With this technique Tuthill, Monnier & Danchi (2001) presented a spectacular image of the exceptionally bright Herbig Be star LkH α 101, showing an asymmetric ring of dust emission around the central object (Fig. 6). This was interpreted by Tuthill, Monnier & Danchi (2001) as the inner dust rim of a flared circumstellar disk tilted slightly out of the plane of the sky. The large size was consistent with a dust evaporation radius only if the inner cavity was optically thin. Subsequent Keck aperture masking imaging of another Herbig Be star (MWC 349) also showed clear disk-like geometry (Danchi, Tuthill & Monnier, 2001). However, these two Herbig Be sources remain the only two for which aperture masking interferometry could be applied.

2.3 Size-Luminosity Diagram

Based on the disk geometry seen by aperture masking for Herbig Be stars, and later confirmed for Herbig Ae disks using “long baseline” infrared interferometry (Eisner et al., 2003, 2004), we are led to consider disk models to explain the interferometry size data. Different classes of disk models can be explored in a simple way using a “Size-Luminosity diagram”. To construct this diagram, the interferometer visibility data is fitted by an emission ring model to represent the inner edge of the disk and this ring radius is compared with the inferred central star luminosity from SED fitting (Fig. 7); in this process, the fraction of light coming from the star and disk must be estimated from an SED decomposition. Monnier & Millan-Gabet (2002) showed that the collective literature data of disk sizes could be best explained by an inner rim of dust surrounding an optically-thin region, giving support to the theoretical ideas of N01 and DDN01. Covering four orders of magnitude in luminosity, the measured sizes of the NIR emitting zone scale mostly as the square root of the stellar luminosity, $R_{\text{rim}} \propto L_*^{1/2}$, as

one would expect from the dust evaporation radius. Moreover, these radii appear to be consistent with a dust evaporation temperature between 1000-1500 K, the precise temperature values depending on grain sizes and radiative transfer effects. The initial size-luminosity diagram, based on “first-generation” interferometry measurements, also showed that some high luminosity sources (Herbig Be stars) had smaller disk sizes that could be consistent with an optically-thick inner disk, while (the very few measured) T Tauri disks seemed broadly comparable to the Herbig Ae disks.

Following the first generation of measurements, larger samples of high quality measurements were collected using the longest baseline interferometers, especially the PTI and Keck Interferometers (Eisner et al., 2004; Monnier et al., 2005; Akeson et al., 2005; Eisner et al., 2005). A summary of these data are reproduced here in Figure 7 (originally published in *Protostars and Planets V*; Millan-Gabet et al., 2007) and allow a detailed examination of disk properties as a function of luminosity beyond the earlier work. We see here that with reasonable assumptions about disk backwarming (see Section 3.3), the inferred dust evaporation temperatures are typically between 1500-2000K even when assuming grey dust; as we shall discuss in more detail later, these high temperatures are somewhat problematic based on laboratory data of real grains. Note that most of these measurements were only done along one position angle of the disk; due to projection effects, the true inner radius might be somewhat larger than that measured.

Another key result from the size-luminosity diagram is a definite departure from the $R_{\text{rim}} \propto L_*^{1/2}$ scaling law for some (but not all!) of the brightest sources in the sample, the Herbig B0-B3 stars: for these sources the measured radii are smaller than the trend of the rest of the sample (see Fig. 7). In other words, they are undersized. Apparently the nature of the dust inner rim and/or the gas inward of the dust rim changes for these very luminous sources. Monnier & Millan-Gabet (2002) first suggested that UV absorption by inner gas could explain undersized disks for the higher luminosity targets. The first serious study of this by Eisner et al. (2004) showed that the inner rim model appears to explain the lower and intermediate luminosity sources, but that the high luminosity sources appear to be better fit with a flat disk (i.e. an inner flat disk of optically thick gas).

The early compendium of sizes showed some puzzling results for T Tauri disks, too. Some T Tauri disk sizes were quite large compared to expectations based on the central star luminosities (e.g., Colavita et al., 2003; Akeson et al., 2005; Eisner et al., 2005). In some cases, the accretion luminosity of the infalling material is comparable to the star’s luminosity and must be included in the total central luminosity. Given the larger errors bars, it seems the disk sizes seem to roughly obey the same relations as Herbig Ae stars once the total central luminosity is included (Muzerolle et al., 2003; Millan-Gabet et al., 2007), but more work is needed with higher angular resolution to improve the measurement precision.

2.4 Beyond size-luminosity relations: Inner disk shapes

The size-luminosity diagram is a simplistic representation of an increasingly large quantity of multi-wavelength, spatially-resolved observations. The diagram embeds a number of assumptions and can hide the effect of important physical processes. New data and modelling have uncovered strong evidence for marked departures from the simple “optically-thin” inner cavity disk model with “puffed-

up” inner wall. The core set of observations are first described here and some of the underlying physical mechanisms are explained and explored further in Section 3.

One of the predictions that the disk inner rim model makes is that the NIR image on the sky should deviate from point-symmetry if the inner rim is seen under an inclination angle that is sufficiently large. As can be clearly seen in Fig. 4, if the dust inner wall is perfectly vertical then this deviation from point symmetry should be very strong: one can only see the far side of the wall, not the near side. If the rim is very much rounded off the situation softens a bit and point symmetry would only be dramatically broken when looking at a relatively large inclination angle. Isella & Natta (2005) and Tannirkulam, Harries & Monnier (2007) both discovered very natural reasons why the rim should be rounded off, as we shall discuss in Section 3.

The IOTA 3-telescope interferometer provided a chance to probe such asymmetries by introducing the possibility of measuring a quantity called the “closure phase” (Monnier, 2007). The closure phase is an observable that is immune to atmospheric turbulence and gives precise information on the disk geometry. If an object is point-symmetric the measured closure phase should be zero, while non-zero closure phase points to deviation from point symmetry. Monnier et al. (2006) reported that only few disks show a strong non-zero closure phase, although half of their 16 sources did show small but significant non-zero closure phase. An analysis showed that these measurements rule out a vertical wall of dust, but are consistent with, and provide support of, the idea of a rounded-off rim.

While models would remain simple if the near-IR emission only emerged from the puffed-up rim, strong evidence is accumulating that there is an additional even hotter component. The first hints came from Eisner et al. (2007) who analyzed narrow-band infrared observations from PTI interferometer and found that the disk sizes showed a small but systematic wavelength dependence. The disk emission region appears to be somewhat smaller at shorter wavelengths than longer ($2.0\mu\text{m}$ compared to $2.3\mu\text{m}$), as would be encountered if there was a hot component contributing to the emission inside the simplistic “dust evaporation” boundary. Indeed, a strict prediction of a hot inner wall model is that the disk emission sizes at different near-IR wavelengths should all be the same. The idea of “hot” emission (maybe gas or refractory dust) inside the main puffed-up inner wall is also suggested by multi-wavelength modeling of interferometry data by Isella et al. (2008) and Kraus et al. (2008).

The proposition of an extra emission component is now secure with recent long-baseline ($\sim 300\text{m}$) data from the CHARA interferometer: the inner regions of the Herbig Ae prototypes MWC 275 and AB Aur cannot be described by just a simple puffed-up inner wall. Tannirkulam et al. (2008) reported two major discoveries using the “record-breaking” 1.5 milliarcsecond resolution data from CHARA: the inner edge of the disk is “fuzzy” and the amount of infrared excess is much greater than expected from traditional SED decomposition into a star + near-IR bump (see Figure 2).

The “fuzzy” inner boundary is inferred from the lack of a visibility “bounce” from the long-baseline CHARA interferometer observations (see Fig. 5) and proves that multiple components must exist in the inner AU of these disks. The high NIR excess ($\sim 85\%$ at $2.2\mu\text{m}$) is probably impossible to generate from a passive disk that simply re-radiates stellar luminosity (see Section 3.8), and points

importantly to a new energy source or to a radically different geometry. These data also prove the scales on which the excess emission arises to be well outside the star’s surface and must be associated with the inner disk (or possibly an inner disk wind?). A more extensive dataset from VLTI on MWC 275 (Benisty et al., in press) gives more details on the inner disk morphology and multi-wavelength properties and also supports the idea that the H and K band emission arises from a broad range of radii (“fuzzy” rim) instead of only a narrow range (“sharp” rim). Note that these data have only been obtained for the brightest Herbig Ae stars and it is unclear whether this “fuzzy” rim is a general feature of most YSO disks (including T Tauri stars) or if this only applies to highly-accreting objects.

In addition to the rich spatial, multi-wavelength data, there are other signs of dynamic and non-trivial physics operating in the inner disk. Wisniewski et al. (2008) and Sitko et al. (2008) report significant changes in the environment of MWC 275 (see further discussions in Section 3.7) that could be related to the the production of the observed jet in this system (Devine et al., 2000). There have also been other reports of inner disk asymmetries in AB Aur (Millan-Gabet et al., 2006) and LkH α 101 (Tuthill et al., 2002).

These recent findings seem to show that, while the inner dust rim picture may be true in its essence, the simple assumption of a completely transparent and non-emitting inner hole inside of a well-defined dust rim is likely to be too naive. The origin of the inner “hot” emission is still a mystery and the theoretical considerations are outlined in Section 4. It might come from accretional energy release in the gas inward of the dust rim (Akeson et al., 2005), or from refractory dust that survives close to the star because it is being “protected” by the gas (Monnier et al., 2005), or even from an inner disk wind/velope. But so far none of these scenarios are conclusive.

New spectroscopic and even spectro-interferometric observations hold immense promise to reveal the origin of this mysterious “hot” inner component. Before summarizing these recent results, we want to re-visit disk theory and tie together all the physical processes we have just been discussing. Following the development of the new “standard disk model” we will come back and discuss the most recent results and future promising avenues of study.

3 Models of the inner dust rim

Motivated by the many exciting observations discussed in the previous section, the presumed inner dust rims have been studied from a theoretical modeling perspective by a number of authors. The main ingredient for this modeling is radiative transfer: the calculation of how the radiation from the star enters the disk, diffuses through it and thus determines the temperature structure of the disk in the region of the dust rim. This problem has proven to be extremely complex, and even as of this writing not nearly the last word has been said on this topic. Let us now “get our hands dirty” by not only reviewing the theoretical models of the last decade, but also by going through some of the math. We will start with the simplest models, those of N01 and DDN01.

3.1 Early “vertical wall” models of the dust inner rim

The earliest models of the dust inner rim, those of N01 and DDN01, were rather primitive. The aim was to get a first order understanding of the origin of the

NIR bump without going into detailed radiative transfer modeling. From basic considerations, for instance by assuming a disk mass of $0.01 M_{\odot}$, the optical depth of the dusty inner disk was expected to be extremely high as long as the dust was present. So the dust inner rim was treated as an optically thick vertical wall at a radius R_{rim} such that the dust in the wall has a temperature of 1500 K, the dust evaporation temperature. Calculating the temperature of a given wall is, strictly speaking, a challenging task. But for these simple initial models it was assumed that the wall radiates like a blackbody, i.e. it emits a flux $F_{\text{cool}} = \sigma T_{\text{rim}}^4$, where σ is the Stefan-Boltzmann constant. This should be compensated by the irradiation of the wall by the star. Here it was assumed that the gas inward of the wall is transparent, so we get $F_{\text{heat}} = L_*/(4\pi R_{\text{rim}}^2)$. Equating the two gives:

$$R_{\text{rim}} = \sqrt{\frac{L_*}{4\pi\sigma T_{\text{rim}}^4}} = R_* \left(\frac{T_*}{T_{\text{rim}}} \right)^2 \quad (1)$$

where in the second identity we defined $T_* = (L_*/4\pi R_*^2\sigma)^{1/4}$. For the parameters of AB Aurigae ($R_* = 2.4 R_{\odot}$, $T_* = 10000$ K) and for $T_{\text{rim}} = 1500$ K we obtain $R_{\text{rim}} = 0.5$ AU.

This tells only half of the story. The other half is to calculate the surface height of the rim $H_{\text{s,rim}}$, because together with the radius it determines the so-called ‘‘covering fraction’’ of the rim, i.e. the fraction of the sky as seen by the star that is covered by the dust in the inner dust rim. This determines the fraction of the stellar light that is captured by the rim and converted into NIR radiation, thus directly determining the strength of the NIR flux. The concept of covering fraction is extremely important for any circumstellar matter that reprocesses the stellar radiation to other wavelengths. While a protoplanetary disk can in principle also produce its own energy through the accretion process, for most cases this is only a small amount compared to the luminosity of the star. So we can safely assume that the disk, and its dust inner rim, is just a ‘‘passive’’ object: it absorbs stellar radiation, and reemits this radiation in the infrared. The total NIR emission from the inner rim is then easily calculated:

$$L_{\text{rim}} \simeq \omega L_* \quad (2)$$

where ω is the covering fraction:

$$\omega \simeq \frac{H_{\text{s,rim}}}{R_{\text{rim}}} \quad (3)$$

where $H_{\text{s,rim}}$ is the surface height of the rim, which we will discuss in more detail below. In the above derivation we assume that all the emitted infrared radiation from the rim escapes the system and none is re-absorbed by the disk. This assumption is approximately valid as long as $H_{\text{s,rim}} \ll R_{\text{rim}}$. For such a simple cylindrically shaped rim the luminosity L_{rim} is very an-isotropic: The observed flux for an observer at infinity at an inclination i is roughly

$$F_{\nu,\text{rim}} \simeq 4 \sin i \frac{R_{\text{rim}} H_{\text{s,rim}}}{d^2} B_{\nu}(T_{\text{rim}}) , \quad (4)$$

for inclinations i small enough that the outer disk does not obscure the view to the inner disk. Here d is the distance to the observer and $B_{\nu}(T)$ is the Planck function at frequency ν and temperature T . Clearly $F_{\nu,\text{rim}}$ from such a simple

cylindrical rim model is zero for $i = 0$, i.e. for face-on view. As already stated above, this simplification has been proven to be inconsistent with observations. Also, the spectrum is assumed to be a perfect Planck curve, which is a major simplification as well.

But what is the value of $H_{s,\text{rim}}$, i.e. How vertically extended is the dust rim? The first thing to do is to make an estimate of the vertical hydrostatic structure of the disk at $R = R_{\text{rim}}$. Let us assume that the temperature of the rim is independent of the vertical coordinate z , measured upward from the midplane. Let us also assume that the disk is geometrically thin, so that $z/R \simeq \cos \theta \simeq \pi/2 - \theta \ll 1$, where θ is the latitudinal coordinate of the spherical coordinate system, being $\theta = 0$ at the pole and $\theta = \pi/2$ at the equator. For a disk rotating with a Keplerian rotation speed $\Omega(R) = \Omega_K(R) \equiv \sqrt{GM_*/R^3}$ (with M_* the stellar mass) each gram of disk material experiences a vertical force $f_z \simeq -\Omega_K^2 z$. The equation of hydrostatic equilibrium $dP/dz = -\rho f_z$ then has the following solution:

$$\rho_{\text{gas}}(R, z) = \frac{\Sigma_{\text{gas}}}{\sqrt{2\pi}H_p} \exp\left(-\frac{z^2}{2H_p^2}\right) \quad (5)$$

where Σ_{gas} is the surface density of the gas: $\Sigma_{\text{gas}} \equiv \int_{-\infty}^{+\infty} \rho(z)dz$ and the pressure scale height H_p is given by

$$H_p = \sqrt{\frac{kTR^3}{\mu_g GM_*}} \quad (6)$$

where $\mu_g \simeq 2.3m_p$ is the mean molecular weight, m_p the proton mass and k the Boltzmann constant. Applying these formulae to $R = R_{\text{rim}}$ and $T = T_{\text{evap}}$ yields $H_{p,\text{rim}}$. For AB Aurigae, our example star with a mass of $M_* \simeq 2.4 M_\odot$, and for $T_{\text{evap}} = 1500$ K we get $H_{p,\text{rim}} \simeq 0.036 R_{\text{rim}}$.

The pressure scale height of the disk at the dust rim, $H_{p,\text{rim}}$, is not necessarily the same as the surface height $H_{s,\text{rim}}$. The rim surface height is defined as the height above which stellar photons can pass substantially beyond R_{rim} without being absorbed. To compute this height we need to know the opacity of the dust in the rim as seen by stellar photons. For small silicate dust grains a typical opacity in the V band would be $\kappa_{\text{sil}}(V) \simeq 10^4$ cm²/gram-of-dust. If we assume a gas-to-dust ratio of 100, then we can estimate that stellar photons that move radially outward along the midplane are absorbed in an extremely thin layer on the surface of the rim: a layer defined by having an optical depth of about unity in the V band. The geometric thickness of this layer is $\Delta R = 100/(\rho_{\text{gas}}\kappa_{\text{sil}})$ which for a gas surface density of $\Sigma_{\text{gas}} = 100$ gram/cm² and a pressure scale height of $H_{p,\text{rim}} = 0.035R_{\text{rim}}$ amounts to $\Delta R \simeq 2.5 \times 10^{-4} H_{p,\text{rim}} \simeq 10^{-5} R_{\text{rim}}$, indeed an extremely thin layer.

Now, ρ_{gas} decreases with height above the midplane. So a stellar photon moving radially outward at an angle φ with respect to the midplane will hit the inner dust wall at a height $z \simeq \varphi R_{\text{rim}}$, where according to Eq. (5) the density is lower, and thus the geometric thickness ΔR of the absorbing layer becomes larger. At some height z , ΔR becomes as large as a few times $H_{p,\text{rim}}$ (in the DDN01 paper it was taken to be 8 times): this is what we can define to be the ‘‘surface height’’ of the rim, $H_{s,\text{rim}}$. In practice $H_{s,\text{rim}}$ is of order 3 to 6 times $H_{p,\text{rim}}$, depending on the surface density Σ_{gas} .

It is important to note here that these are all rough estimates, and by no means detailed calculations. As we shall see shortly, the problem of radiative transfer in

the rim, i.e. the determination of the temperature structure, and thus the vertical hydrostatic structure of the rim is a very complex problem.

3.2 Temperature of individual dust grains in the dust rim

By assuming the rim to behave like a solid blackbody wall we have totally ignored the individual particle character of the dust grains. Let us first calculate the temperature of a single dust grain located at a distance R from the star in a completely optically thin environment. If we assume that the dust grain is a sphere of radius a and that the optical absorption cross section equals its geometric cross section πa^2 (amounting to a “grey opacity”, i.e. an opacity independent of wavelength), then the total amount of energy that the grain absorbs per second is $\pi a^2 L_*/4\pi R^2$. If the grain has a temperature T_{grey} , then it emits blackbody radiation all over its surface, amounting to a cooling rate of $4\pi a^2 \sigma T_{\text{grey}}^4$. Equating the two yields:

$$T_{\text{grey}} = \left(\frac{L_*}{16\pi\sigma R^2} \right)^{1/4} = \left(\frac{R_*}{2R} \right)^{1/2} T_* \quad (7)$$

If we put in the same numbers as we did before, for AB Aurigae, then we get at $R = R_{\text{rim}} \simeq 0.5$ AU a grey dust temperature of $T_{\text{grey}} = 1050$ K, i.e. substantially smaller than the 1500 K we calculated on the basis of the solid blackbody wall assumption. So what has gone wrong? One of the problems is that we did not include the “backwarming” of our dust grain by the thermal emission from the dust further inside the wall. But a more precise analysis shows that we can only do this properly if we solve the equations of radiative transfer in the disk rim, as we shall do in Section 3.3. Moreover, our assumption of a grey dust grain, i.e. a dust grain with a wavelength-independent opacity, is likely to be wrong as well. By accounting for the full opacity law κ_ν (see Fig. 8) we obtain the following equation for the dust temperature of a single grain at distance R from the star:

$$\int_0^\infty \kappa_\nu F_{*,\nu} d\nu = 4\pi \int_0^\infty \kappa_\nu B_\nu(T_{\text{dust}}) d\nu \quad (8)$$

where $F_{*,\nu} = L_{*,\nu}/4\pi R^2 = \pi(R_*/R)^2 B_\nu(T_*)$ is the flux from the star which we assume here, for convenience, to be a blackbody emitter. Solving this equation for T_{dust} can be done numerically. We can write Eq. (8) in a way very similar to the grey case, but with a correction factor:

$$T_{\text{dust}} = T_* \frac{1}{\epsilon^{1/4}} \sqrt{\frac{R_*}{2R}} \quad (9)$$

where ϵ is defined as

$$\epsilon \equiv \frac{\int_0^\infty \kappa_\nu B_\nu(T_{\text{dust}}) d\nu / T_{\text{dust}}^4}{\int_0^\infty \kappa_\nu B_\nu(T_*) d\nu / T_*^4} \quad (10)$$

The symbol ϵ tells what is the ratio of effectiveness of emission at wavelength at which the dust radiates away its heat and absorption at stellar wavelengths. This ratio depends on the value of T_{dust} itself, so Eq. (9) is an implicit equation and requires numerical iteration to solve (each time updating the ϵ value). But it does tell us something about the radiation physics involved. For the case of $\epsilon < 1$ the stellar light (being at high temperatures and thus short wavelengths) is absorbed at wavelengths where the opacity of the dust is large, while the dust,

being less than 1500 K in temperature, cools at wavelengths where the opacity is smaller. This means that if $\epsilon < 1$ one has $T_{\text{dust}} > T_{\text{grey}}$ while for $\epsilon > 1$ one has $T_{\text{dust}} < T_{\text{grey}}$. The “efficiency factor” ϵ therefore tells how efficiently the dust can cool. For κ_ν increasing with ν , as is typical for small ($a \lesssim 1\mu\text{m}$) grains (see Fig. 8), we have $\epsilon < 1$. Grains that are substantially smaller than 1 micron in radius have a small efficiency factor, $\epsilon \lesssim 0.5$, while grains larger than about ten microns have an efficiency factor close to unity, $\epsilon \simeq 1$. This means that if the dust rim consists of small grains only, we expect its inner radius to lie further out than if the rim consists of large grains. This can in fact be seen in the 2-D/3-D models described in Section 3.6. In other words: large grains can survive closer to the star than small grains.

Presumably crystalline grains can also survive closer to the star than amorphous grains. In fact, dust at temperatures close to the sublimation temperature is expected to be crystalline rather than amorphous as in Fig. 8. Pure crystals, even if they are very small, will have a very low opacity in the V band and thus their “efficiency factor” ϵ may be much larger than unity, allowing them to survive close to the star. The question is, however, how pure such crystals are in reality, and if they are in thermal contact with iron grains (which have a very low ϵ , hence high temperature).

3.3 An approximate 1-D radiative transfer model of the dust rim

Now let us come back to the issue of backwarming, i.e. the effect of mutual heating of the grains by exchange of thermal radiation. Solving the full set of radiative transfer equations in a dust rim would require at least a 2-D treatment of the problem, as we shall discuss in Section 3.6. This is a complex problem. But even a 1-D horizontal approximation to the radiative transfer problem in the inner rim is sufficiently complex that a full treatment requires a numerical approach. Without going into any further detail, let us simply present a formula for the dust temperature as a function of radial optical depth that approximates the result of a full 1-D treatment reasonably well (Isella & Natta 2005; D’Alessio et al. 2004; Muzerolle et al. 2003; Calvet et al. 1991):

$$T_{\text{dust}}(\tau_d) = T_* \sqrt{\frac{R_*}{2R}} \left[\mu(2 + 3\mu\epsilon) + \left(\frac{1}{\epsilon} - 3\epsilon\mu^2 \right) e^{-\tau_d/\mu\epsilon} \right]^{1/4} \quad (11)$$

where τ_d is the optical depth as measured at wavelengths near the peak of the Planck function for the dust temperature (for our inner rim analysis this would be around 1500 K) and $\mu = \sin \phi$ with ϕ being the angle under which the stellar radiation enters the dust wall. For stellar radiation entering the wall near the equatorial plane, and thus perpendicularly, one has $\phi = \pi/2$, i.e. $\mu = 1$. On the other hand, if one would choose $\mu = 0$ and $\tau_d = 0$, one recovers the equation for a single dust grain without any nearby matter, Eq. (9). The extra terms that appear for $\mu > 0$ have to do with the backwarming effect due to emission from other grains, and the $e^{-\tau_d/\mu\epsilon}$ factor has to do with the extinction of the direct stellar light as it penetrates deeper into the rim. Note, by the way, that Eq. (11) assumes that $\epsilon = \text{constant}$, which is of course just an approximation.

Now let us plot the solutions for the parameters of AB Aurigae for different values of ϵ (Fig. 9). For the moment we will ignore the issue of evaporation or condensation of dust. The x-axis is plotted logarithmically, so the absolute inner edge of the dust is at $\log(\tau_d) = -\infty$, i.e. infinitely much to the left of the graph.

For $\epsilon = 1$ the dust near/at the inner edge (left part of the graph) has a lower temperature than the dust deep inside the dust rim (right part of the graph). The cause of this effect is a bit subtle, but it can be traced back to the mutual radiative heating of the dust grains deep in the rim: the infrared radiation that one grain emits can be absorbed by another grain. This is the “backwarming” we mentioned earlier. A grain at $\tau_d \gg 1$ is immersed in this radiation field, while for a grain at $\tau_d \ll 1$ only half of the sky is delivering dust infrared emission. On the other hand, that dust grain sees the stellar radiation field. For $\epsilon = 1$, however, the effect of mutual heating is stronger than the direct stellar radiative heating, hence the larger temperature deeper in the rim. A more detailed analysis would require some form of radiative transfer, for instance the two-ray treatment explained in chapter 1 of the book by Rybicki & Lightman (1979).

The situation is reverse for the cases of $\epsilon = 0.1$ and $\epsilon = 0.3$ shown in the figure. There the dust at the very inner edge is quite hot (1960 K if we ignore evaporation for the moment) while it is much cooler deeper inside the rim (1300 K). This is because the dust that is in plain sight of the star sees radiation that is very hot, and heats the grains at wavelengths where κ_ν is much larger than at NIR wavelengths where the grain cools. Heating is then more efficient than cooling, and thus the dust becomes “superheated”. Deep in the disk, however, there is no stellar light available and this superheating effect is gone, hence the lower temperature on the right side of the graph.

For a critical value of the efficiency parameter, $\epsilon = 1/\sqrt{3}$, the temperature is constant with τ_d . Here all effects exactly cancel and there is no temperature difference between the front and the back side of the wall. This critical value of ϵ divides two very distinct kinds of inner dust rim solutions, as was discovered by Isella & Natta (2005). These solutions show that the dust rim is rarely a single-temperature object, as was pointed out by Muzerolle et al. (2003).

3.4 Is the rim a sharp, well-defined evaporation front?

The reader may have already been bothered in the above radiative transfer analysis by the fact that for all solutions except one there are regions where the dust temperature exceeds the dust evaporation temperature of 1500 K. So what does this mean? For the low- ϵ solutions, with high temperatures at the inner edge, this means that the star will simply evaporate the dust and gradually “eats its way” outward into the disk, moving the dust rim (and thus the above solution) outward until, through the geometric $1/R^2$ dilution effect, the superheated dust temperature arrives at the dust evaporation temperature. In other words: the inner rim of a disk that consists of small $a \ll 3\mu\text{m}$ grains is likely to lie at radii larger than that predicted by Eq. (1). In fact, this radius can be easily estimated, as long as $\epsilon \ll 1/\sqrt{3}$: under those conditions the contribution of the backwarming by the grains deeper in the rim becomes negligible and one can simply use Eq. (9) and arrive at

$$R_{\text{wall}} \simeq R_* \left(\frac{T_*}{T_{\text{evap}}} \right)^2 \frac{1}{2\sqrt{\epsilon}} = \frac{R_{\text{wall,bb}}}{2\sqrt{\epsilon}} \quad (12)$$

where $R_{\text{wall,bb}}$ is the inner rim radius given by Eq. (1). So the dust rim radius for small grains is larger than that predicted by DDN01 if $\epsilon < 0.25$. Right behind the new location of the inner dust wall the temperature drops dramatically, and over a very tiny spatial scale (remember the estimations of ΔR earlier). The dust

wall will thus have a flimsy layer of hot dust covering its inner edge, but will be much cooler inside.

Now let us investigate what happens for $\epsilon > 1/\sqrt{3}$. It appears from Fig. 9 that the grains on the inside of the wall are below the evaporation temperature while those deep inside heat each other up beyond the evaporation temperature. This gives rise to a very confusing situation: all the dust deep inside the rim would evaporate while the dust on the very inner edge would remain. This makes it impossible to define a clear-cut location of the evaporation front. If we would include 2-D/3-D radiative transfer effects (see Section 3.6) things would become a bit less extreme, because radiation behind the dust rim can escape vertically and thus cool down the regions some distance behind the rim. But we would still face the confusing situation that we cannot make a clean definition of where precisely the transition is between the hot inner dust-free disk and the cooler outer dusty disk.

There are ideas floating in the literature on how Nature may solve this apparent paradox. One is that instead of a sharply defined evaporation front (a two-dimensional surface) we have what we could call a “translucent rim”: a three-dimensional volume of roughly optical depth unity, in which the fraction of evaporated dust gradually increases from 0 to 1 as one moves inward toward the star. This was predicted by Isella & Natta (2005) and Vinković (2006) based on 1-D models, and something similar to this was later indeed found in 2-D models by Kama, Min & Dominik (2009). For the 2-D multi-grain size models of Tannirkulam, Harries & Monnier (2007), however, no such translucent rim was found. Progress in this area is, however, rather slow because it appears evident that the solution of this problem lies in the interplay between the complex physics of dust evaporation and condensation with the numerically challenging problem of 2-D/3-D radiative transfer (Section 3.6). It appears therefore that the issue of how the evaporation front looks is still a wide open question for future theoretical research.

3.5 Better treatment of dust evaporation: a rounding-off of the rim

So far, in our analysis of the dust rim, we always assumed a single temperature at which the dust evaporates. This is, however, a simplification with far reaching consequences, as Isella & Natta (2005, henceforth IN05) found out. In reality, whether dust exists or not depends on a balance of the processes of evaporation and condensation. While the evaporation rate per unit area on grain surfaces depends on temperature only, the rate of condensation depends also on the abundance of condensable atoms and molecules in the gas phase. Typically, at a given temperature there is an equilibrium partial pressure of vapor for which the evaporation and condensation cancel each other out. If the partial pressure of the vapor is below that value, any available solid state dust will continue to evaporate until either the partial pressure of the vapor has reached the critical vapor pressure or all the solids have been evaporated away. The process of evaporation and condensation can be quite complex (Section 3.9), but if the abundances of condensable atoms and molecules are known, it roughly amounts to having a temperature-dependent critical total gas pressure $P_{\text{gas,crit}}(T)$ above which dust can exist in solid form and below which it cannot. In other words, for a given gas density, there exists a critical temperature T_{evap} above which the dust evapo-

rates and below which it will condense. IN05 give a fitting formula of the tabular results of Pollack et al. (1994) which reads: $T_{\text{evap}} = G\rho_{\text{gas}}^\gamma$ in which ρ_{gas} is given in units of gram per cm^3 and the constants are $G = 2000$ and $\gamma = 0.0195$. The dependence of T_{evap} on density is weak, but since the density drops by a huge factor over a few pressure scale heights (cf. Eq. 5) the evaporation temperature drops considerably with height above the midplane. Adopting small dust grains and thus using Eq. (12) as an estimate of the evaporation radius as a function of z , and using Eq. (5) for the vertical gas density distribution, we arrive at the following shape of the disk rim:

$$R_{\text{rim}}(z) \simeq R_* \frac{T_*^2}{2G^2\sqrt{\epsilon}} \left(\frac{\Sigma_{\text{gas}}}{\sqrt{2\pi}H_{\text{p,rim}}} \right)^{-2\gamma} e^{\gamma z^2/H_{\text{p,rim}}^2} \quad (13)$$

We must make an estimation of $H_{\text{p,rim}}$ and Σ_{gas} even though the radius at which we should estimate them would in principle depend on the outcome of the calculation itself. For AB Aurigae, assuming $\Sigma_{\text{gas}} = 100 \text{ gram/cm}^2$ and small grains, say, grains with $\epsilon = 0.1$, the midplane rim radius for this model lies roughly around 1.0 AU. If we use the $\tau_d \rightarrow \infty$ temperature from Eq. (11) for our chosen value of ϵ (taking $\mu = 1$), we get a temperature from which we can obtain, through Eq. (6), a reasonable estimate of the pressure scale height $H_{\text{p,rim}}$ behind the rim. In our example this becomes $H_{\text{p,rim}} = 0.044 \text{ AU}$. With Eq. (13) we can now calculate that the rim midplane radius is 1.1 AU, roughly confirming our Ansatz of 1 AU. The resulting rim shape is plotted in Fig. 10.

The figure shows that the rounding-off of the rim is very strong. This is not an effect that can be conveniently ignored. The figure also shows the height above the midplane where the rim becomes optically thin (the dashed line), showing that the rim can have $H_{\text{s,rim}}$ as large as 0.2 AU, which in this case amounts to a covering fraction of about 20%, i.e. producing an inclination-averaged NIR luminosity of $L_{\text{NIR}} \simeq 0.2 L_*$. The dust evaporation temperature in the rim ranges from 1270 K near the midplane down to 1050 K at the point where the rim becomes optically thin. These dust evaporation temperatures are smaller than the 1500 K assumed usually, and this may lead to the model bump peaking at slightly longer wavelengths than observed (Isella et al. 2006). But these results depend on the minerals one assumes and on grain sizes. In fact, as we shall see in Section 3.6, grain size distributions may also result in the effect of rounding-off of the rim, in addition to the IN05 mechanism.

3.6 Two-dimensional radiative transfer models

To get deeper into the issue of the 2-D shape of the rim and the region just behind it, it is clear that there is no path around utilizing 2-D continuum radiative transfer codes. With “2-D” we actually mean 3-D, in the sense the light is allowed to move in all 3 spatial directions. But the dust temperatures and other quantities that result from these calculations have axial symmetry: they only depend on the coordinates R and z . In that sense these models are clearly 2-D.

The problem of multi-dimensional radiative transfer can only be solved using numerical methods. There are basically two main types of radiative transfer algorithms in use today: those based on iterative integration of the formal transfer equation along pre-defined photon directions (so called “grid based codes” or better “discrete ordinate codes” because the angular directions are modeled as

an angular grid) and those based on a Monte Carlo type of simulation of photon movement. In 1-D the discrete ordinate methods have proven to be extremely efficient and usually superior over Monte Carlo methods. But in 2-D and 3-D the discrete ordinate methods become cumbersome and difficult to handle. Moreover, many of the advantages of these methods are lost in 2-D and 3-D. Therefore, for problems of multi-dimensional continuum radiative transfer in circumstellar disks and envelopes the Monte Carlo method has become the most popular method. In particular the Monte Carlo methods of Lucy (1999) and of Bjorkman & Wood (2001) have proven to be ideally suited for this problem, and by far most models today use these techniques or variants of them. These methods are robust (they give reasonable answers even for non-expert users) and easy to handle. The main drawback is that in very highly optically thick regions these codes can become slow and/or give low photon statistics and hence high Monte Carlo noise. Improvements in the efficiency of these methods, however, have made this problem less serious in recent years (see e.g. Min et al. 2009 and Pinte et al. 2009).

The first 2-D frequency-dependent radiative transfer treatment of the inner rim problem was presented, in the context of full disk models, by Dullemond & Dominik (2004, henceforth DD04a, though see also Nomura 2002). These models gave new insight into the actual appearance of the dust rim and the possible shadow it casts on the disk behind it (see Sections 3.7 and 3.8).

A main concern of the DD04a models is that they did not treat the rounding-off of the rim. Unfortunately the 2-D radiative transfer treatment of a rounded-off rim has proven to be a tremendous challenge, even today. The reason is the extremely thin $\tau_* = 1$ layer at the inner edge of the rim (i.e. $\Delta R \ll R_{\text{rim}}$). For proper radiative transfer one must spatially resolve the transition between optically thin and optically thick. This requires tremendously fine grid spacing at the inner rim. For an inner rim that is aligned with the grid (a vertical rim for cylindrical coordinates) this can be easily achieved by choosing an R -grid that becomes finer and finer close to the rim, as is done in DD04a. But a rounded-off rim is not aligned with the grid. This requires a grid refinement that is not separable in R and z , for instance by allowing cells to be recursively split into 2×2 (or in 3-D $2 \times 2 \times 2$) subcells there where high spatial resolution is required. Such a technique is often called “adaptive mesh refinement” (AMR). While some codes are technically able to do this, there are still various numerical complications that arise with the dust evaporation on such extremely refined grids.

The first successful model of a rounded-off rim with 2-D radiative transfer was presented by Tannirkulam, Harries & Monnier (2007) (Fig. 11). They employed AMR, allowing them to properly follow the very sharp edge of the rounded-off rim. Moreover, they discovered that grain growth and settling could be another source of rounding off of the inner rim, because big grains tend to sediment toward lower z and thus the grains that can survive closer toward the star will be primarily found closer to the midplane. This effect does not replace the IN05 effect, but adds to it.

A recent paper by Kama, Min & Dominik (2009) also studied the rounded off rims with full 2-D radiative transfer, treating the dust evaporation and condensation physics in more detail than IN05. These models confirm various aspects of the the IN05 model: the sharp rims for grains with low cooling efficiency (small ϵ) and the general shape for such rims, the appearance of translucent rims for high- ϵ grains and the general location of the rim. They find that their models that consist of both small and large grains yield structures that are more like

gradually fading disks toward smaller radii than a sharply defined dust rim, as is shown in Fig. 12 (Kama et al. 2009; see also Pontoppidan et al. 2007 discussing rims with mixed dust sizes, though that is a simpler model) .

Clearly, the development of truly 2-D (or even 3-D) self-consistent radiative transfer models of the dust rim for various dust distributions has just begun, and much still needs to be done. But this requires very powerful radiative transfer tools and quite a bit of work to handle them, in particular with the complex numerical difficulties arising due to the evaporation and condensation physics.

3.7 To shadow or not to shadow? The debate on “puffed up inner rims”

So far we have discussed the rim structure rather independently from the rest of the disk behind it. So how do they connect? In the N01/DDN01 papers it was suggested that the rim may have a thicker geometry than the disk directly behind it because as a result of the direct frontal irradiation it is much hotter than the flaring disk behind it that is only irradiated under a shallow grazing angle (see the paper by Chiang & Goldreich 1997 for a nice treatment of flaring protoplanetary disks and the grazing angle irradiation treatment). The inner rim was thus expected to be “puffed-up” compared to the disk directly behind it. This would inevitably lead to the rim casting a shadow over at least the inner few AU of the flaring disk. At larger radii the disk would then “pop up out of the shadow” again and continue outward as a normal flaring disk. While DDN01 recognized that due to radial radiative diffusion this shadow would not be infinitely deep, a relatively strong shadow was nevertheless predicted.

The 2-D calculations of DD04a confirmed the existence of some form of shadow covering the inner few AU of the disk, and depending on the distribution of matter in the disk this shadow could extend even further and in principle engulf the entire disk (“self-shadowed disks”). The paper showed that self-shadowed disks have weaker far-infrared (FIR) flux than flared disks, and confirmed the idea originally put forward by Meeus et al. (2001) that the observed families of weak and strong FIR Herbig Ae/Be sources could be explained in this context.

But it was also found that the shadows were much less pronounced than predicted in the DDN01 model. The radiative diffusion of heat through the disk in radial direction was much more efficient than predicted by DDN01, preventing the shadowed region from cooling substantially. Indeed, Boekel, Dullemond & Dominik (2005) showed that in the mid-infrared the shadowed region was merely a slight dip in the intensity profile between R_{rim} and $4R_{\text{rim}}$.

A debate ensued whether what was claimed to be a “shadow” in the DD04a paper truly matches the definition of shadow, or whether the weak FIR flux is merely an effect of the lower surface densities at larger radii in the “self-shadowed” models (Wood, 2008). The strictly vertical wall in DD04a certainly makes the shadow effect stronger than it would be for a smoother rounded-off rim. Also, even if a shadowing effect takes place, such a shadow is not “sharp” because the top surface of the dust rim is itself presumably somewhat fuzzy. Finally, due to scattering and radial radiative diffusion, radiative energy can seep into the shadowed region, preventing it from cooling drastically. These shadows are therefore certainly not efficient enough to cause the disk behind the rim to hydrodynamically “collapse” toward the midplane for lack of gas pressure support. Even a small amount of radiative diffusion is enough to heat the midplane of the shad-

owed region enough to prevent this. The word “shadow” in this context should therefore be used with care, but can still be useful to explain certain phenomena in protoplanetary disks.

One argument in favor of some form of self-shadowing taking place in some objects is the observation of rapid variations in scattered light images of the outer disk of the Herbig Ae star MWC 275 (Wisniewski et al., 2008). The time scale of a few years is by far too short to be explained by hydrodynamic phenomena in the observed outer disk, which is several hundreds of AU in radius. Interestingly, Sitko et al. (2008) report variability in the NIR for this source while the stellar flux remains steady. This suggests a variable height of the dust rim which might be linked to variable shadowing of the outer disk. A similar effect can be observed in the thermal mid- and far-infrared emission from the outer regions of these disks. For instance, Juhász et al. (2007) have observed variability in the far-infrared in the source SV Cephei measured with IRAS on clearly too short time scales to be consistent with hydrodynamic variability in the far-IR emitting regions. Variable shadowing appears the only viable explanation (Juhász et al., 2007). And recently Muzerolle et al. (2009) made multi-epoch Spitzer observations of the T Tauri star LRL 31 and found clear differences in the spectra at all epochs. The mid- to far-IR flux varied by 30% over time scales as short as one week. In fact, when the near infrared flux is at its weakest, they found the mid- and far-infrared flux to be the strongest and vice versa. This strongly suggests that some rim of variable height casts a shadow over the outer disk when it is at maximum height, while it leaves the outer disk exposed to irradiation if it is at minimum height. One problem is, however, that Muzerolle et al. (2009) found that at one epoch there is nearly no NIR excess at all, suggesting that the inner rim has disappeared completely at that time. It is unclear how this can have happened.

As mentioned before, however, it is still a matter of debate whether a hydrostatic dust rim can cast such a shadow. There are, however, other ideas discussed in the literature on how to create puffed-up inner rims. Already long before the inner dust rim debate, Bell et al. (1997) found in their models of strongly accreting disks that the inner disk may be puffed-up due to the injection of viscous heat deep inside the disk. Since most of the release of heat happens deep inside the potential well, this puffing up predominantly affects the inner few AU of the disk, and may cause this inner disk to cast a shadow of the outer disk. A similar result was found by Terquem (2008) for disks with deadzones, where it is not the heat injection, but the matter storage in the deadzone that puffs the inner disk up. Conversely, in the models of D’Alessio et al. the midplane heating puffs up the disk behind the rim enough to prevent self-shadowing (N. Calvet, priv. comm.).

3.8 Can the dust rim explain the NIR bump?

We should now go back and ask whether the dust inner rim model can indeed explain the observed NIR bump. The answer is still not conclusive. In contrast to the simpler N01/DDN01 models, the DD04a models appear to predict an overall shape of the NIR bump that is flatter (less “bump like”) and weaker than what is often observed in Herbig Ae stars. The same was found by Tannirkulam et al. (2008a) and Isella et al. (2008). Vinković et al. (2003) were the first to point out this problem. They made a detailed follow-up study of this problem in Vinković et al. (2006) and suggest that for sources with a strong NIR flux, in addition to a disk rim, there must be a second component such as a spherical

envelope that contributes to the NIR flux.

So why did the old models work better in fitting the NIR bump than the more realistic new ones? This is because they are simple single-temperature “blackbody wall” models. From Fig. 2 one can see that a pure blackbody curve fits the bump remarkably well. The more sophisticated models, however, show that the temperature dispersion in the wall smears out the flux in the wavelength domain, making the bump flatter and weaker. To fix the weakness problem we would need to make the rim geometrically thicker so that it can capture a larger portion of the stellar light, and thus become brighter in the NIR (cf. Eqs. 2, 3). Increasing the pressure scale height of the disk is difficult: the temperature is more or less fixed (around 1500 K) and with the radius R and the stellar mass M_* the pressure scale height is given, i.e. there is no room for manoeuvring. Alternatively, by putting far more matter in the rim, the optical surface moves to a higher elevation above the midplane. But it may require more density increase than is realistic. Another idea is to drive a disk-wind that drags along dust and thus adds an extra dust halo around the disk (Vinković & Jurkić, 2007).

An alternative explanation, for which there appears to be evidence from NIR interferometry, is the presence of bright emission from the gas inside the dust rim (Akeson et al. 2005; Monnier et al. 2005; Tannirkulam et al. 2008b; Isella et al. 2008; Kraus et al. 2008). The question is, how can one power this emission without removing power from the dust rim? After all, the gas may capture stellar radiation, but will also shadow the dust rim behind it. One suggestion is that active accretion heats up the disk and thus injects the required additional energy. The other is that if the gas disk extends down to just a few stellar radii, the finite size of the star allows it to radiate down onto the disk and thus increase the covering fraction beyond the simple $\omega = H_s/R$ estimate (see e.g. Friedjung 1985). But the issue of opacity of the gas inward of the dust rim is still very much unclear, as we shall see in Section 4.

3.9 Behind the wall: a dust chemical reactor

The shape, radius and near-infrared emission of the dust inner rim depends critically on properties of the dust such as grain sizes and composition. These are not easy to calculate ab-initio because there are many processes taking place in the dust inner rim that strongly affect these. In fact, the region just behind the dust inner rim can be regarded as a powerful dust chemical reactor. Amorphous dust grains get annealed and thus acquire crystalline structure (Gail 1998); iron may be expelled from the silicates, thus changing the optical properties of these silicates dramatically (Gail 2004); the iron may form pure iron grains for which the opacities are hard to calculate; carbon dust may combust and thus get lost to the gas phase (Gail 2002).

In addition to these chemical processes, the high temperatures also provide for interesting physics to occur. For instance, dust particles that collide at these high temperatures may stick and melt together due to processes such as sintering and/or eutectic melting (see e.g. Blum & Wurm, 2008). This may aid the growth of grains in these rims, meaning that maybe these rims are rich in large molten-together grain clusters. While large grains or grain clusters can exist closer to the star than small grains, if they evaporate nevertheless (for instance due to a temporary fluctuation in the brightness of the star due to some transient accretion event), they will not be able to recondense at those radii because their growth

has to pass through a phase of small grains, and these small grains would only survive at larger radii. Large grains can then only re-appear in these regions if they are transported inward from larger radii.

All of these effects have relevance also for the rest of the disk. The thermally processed material that is created here in this hot “oven” may be partially transported outward to the planet- and comet-forming region of the disk, for instance through radial mixing (e.g. Gail 2001; Bockelée-Morvan et al. 2002). There is evidence for this from ingredients found in the material brought back from comet Wild-2 (Zolensky et al., 2006) as well as from infrared observations (e.g. van Boekel 2004). The study of the dust inner rim is thus also the study of an important preprocessing factory of protoplanetary building material. Clearly there is still a lot to be investigated in this field.

4 Gas inward of the dust rim

One of the main assumptions in the inner dust rim model is that the gas inward of the rim is optically thin, so that the star can freely illuminate the dust rim. However, this assumption is rather crude. Already soon after the first dust rim models came out, Muzerolle et al. (2004) made an investigation of the gas optical depth inward of the dust rim, and they found that for low accretion rates the inner gas is sufficiently transparent for the dust rim to be appreciably illuminated by the star. For high accretion rates ($\dot{M} \gtrsim 10^{-8} M_{\odot}/\text{year}$) they found that the inner gas disk becomes optically thick. However, with recent progress in observational studies of the gas inward of the rim (Section 5) this topic may need to be revisited. In this section we shall discuss current understanding of the dust-free inner disk, thereby moving our attention closer toward the star. We will follow largely the study of Muzerolle et al. (2004).

4.1 Gas opacities

The first thing to do is to get a grasp of the gas opacities at temperatures between T_{\star} and T_{rim} (or even slightly below that) and densities appropriate for our purpose. One may be tempted to use one of the publically available tables of Rosseland- or Planck-mean gas opacities available on the web. But such opacities are valid only in optically thick media, or in media of medium optical depth ($\tau \sim 1$) that are not irradiated by an external source. In our case we expect that neither of these conditions are met. At low accretion rates the gas will be at least partially optically thin, and it will be strongly irradiated by the light of the star, which has a color temperature much in excess of the gas kinetic temperature. We are therefore forced to use some form of frequency-dependent opacities. In most cases the gas is at too low temperatures for strong continuum opacity sources such as H^{-} to play a substantial role, except in the very tenuous surface layers of the disk where temperatures may be very high (Glassgold, Najita & Igea, 2004). Instead, depending on the local chemistry, we may be faced with a zoo of billions of molecular and atomic lines. An example of such a zoo is shown in Fig. 13, which was calculated for a temperature of about 2000 K and a density of $\rho_{\text{gas}} \simeq 4 \times 10^{-9} \text{ g/cm}^3$, and based on chemical equilibrium abundances of molecular and atomic species.

Whether the actual gas opacity of the dust-free inner disk is as rich in molecular lines as the opacity shown in Fig. 13 is, however, not clear. Molecules are

fragile and are collisionally destroyed at temperatures much in excess of 2500 K. Moreover, UV photons from the star and from the accretion shocks near the stellar surface can photodissociate these molecules even if they are well below the thermal dissociation temperature. The destruction of molecules, if it proceeds all the way to atoms, would clearly reduce the opacity dramatically. For H₂O the problem of photodissociation in dust-depleted surface layers of disks has been studied by Bethell & Bergin (2009). They found that water is quite efficient in shielding itself from the destructive UV photons of the star. And Glassgold, Meijerink & Najita (2009) suggest that the more the dust is removed from the disk, the stronger the observed infrared H₂O lines should become. But none of these models are directly applicable to the very inner dust-free disk, and their physics and chemistry is still far from complete. Clearly a lot still has to be investigated before a good picture emerges of the composition and opacity of the gas inward of the dust rim.

If we, for now, take the opacities of Fig. 13 at face value, then one is faced with the question how to deal with the complexity of it, involving billions of molecular lines. While the opacity can be very high at the line centers, there are opacity valleys between lines, so radiation can seep through these “leaks”. And there are regions with few or no lines where, because there is (by assumption) no dust inside of the dust inner rim, there is only a weak gas continuum opacity present. This is particularly so for the region between about 0.2 and 0.4 μm . Stellar radiation is allowed to pass virtually unhindered through such a “window”. There is no ultimate answer to the question how to handle this complexity. But by assuming that all abundances and excitations of the molecules are in local thermodynamic equilibrium (LTE) and by using techniques such as “opacity sampling” (Ekberg, Eriksson & Gustafsson, 1986) or multi-group methods (Mihalas & Mihalas 1984), progress can be made.

Another method, employed by Muzerolle et al. (2004), is to treat the large opacity gap between 0.2 and 0.4 μm (Fig. 13) separately from the rest, and treat the rest using special-purpose mean opacities, constructed particularly for the problem at hand. Let us now have closer look at that paper.

4.2 Structure of the dust-free gas inner disk

Muzerolle et al. (2004, henceforth MDCH04) used the basic framework of disk structure of the D’Alessio disk models (D’Alessio et al. 1998; Calvet et al. 1991) and replaced the dust opacities with the appropriate gas mean opacities to obtain a model of this part of the disk. To overcome the problems with the use of mean opacities, they constructed a specially tailored mean opacity which acts as a Planck mean, but takes into account the opacity gaps between the lines in the $\lambda > 0.45\mu\text{m}$ regime. For $0.2 < \lambda < 0.45\mu\text{m}$ they assume appropriately weak continuum opacity. In this section we will construct a simplified version of that model as an illustration of the gas inner disk issue.

Following MDCH04, we use a razor-thin disk approach, so that the irradiation of the disk by the star occurs solely due to the finite size of the star, allowing it to shine down on the disk. The average angle under which this radiation then hits the disk is

$$\varphi(R) \simeq \frac{4}{3\pi} \frac{R_*}{R} \quad (14)$$

We also assume that only the upper half of the star surface is able to radiate

onto the upper surface layers of the disk (MDCH04 put this additional factor of 1/2 inside their definition of $\varphi(R)$). MDCH04 found that at these very shallow angles the stellar radiation longward of $0.45\mu\text{m}$ will be fully absorbed by the surface of the gas disk. They also found that for small enough accretion rate the temperature of this surface layer is always around 2000 K. Now following the reasoning of Chiang & Goldreich (1997) this layer re-emits the absorbed energy at its own temperature (2000 K), producing emission in the NIR. Half of this radiation is lost upward, the other half is radiated downward into the disk. At these wavelengths the opacity of the gas hovers between $\kappa_\nu \sim 10^{-2}$ and $10^1 \text{ cm}^2/\text{g}$ (cf. Fig. 13, but keep in mind the caveats). Below we will verify whether the gas disk is optically thick in vertical direction at all these wavelengths; for now we make this assumption and find, by balancing the downward flux $F_{\text{down}} = (1/4)f\varphi(R)L_*/(4\pi R^2)$ (with f explained below and the factor 1/4 accounting for the two factors 1/2 discussed above) with upward the cooling flux $F_{\text{up}} = \sigma T_{\text{mid}}^4$ that the midplane temperature is

$$T_{\text{mid}} = T_* \sqrt{\frac{R_*}{R}} \left(\frac{1}{4}f\varphi(R)\right)^{1/4} = \left(\frac{R_*^3 f}{3\pi}\right)^{1/4} T_* R^{-3/4} \quad (15)$$

where again we assumed $L_* = 4\pi R_*^2 \sigma T_*^4$ for simplicity. The factor f tells how much of the stellar radiation is longward of $0.45 \mu\text{m}$. Let us take this factor to be 1/2. This estimate does not include the heating effect by viscous accretion in the disk. According to MDCH04's solutions, however, this only kicks in for accretion rates $\dot{M} \gtrsim 3 \times 10^{-8} M_\odot/\text{yr}$, so we will ignore this here. One can now plot the above result and compare to Fig. 9 of MDCH04 to find that the match is not bad for the cases of $\dot{M} \lesssim 10^{-8} M_\odot/\text{yr}$.

With this estimate of the temperatures of the midplane and the surface layers of the gaseous dust-free inner disk, we can calculate the surface density in the disk. We need standard Shakura-Sunyaev-type accretion disk theory (see e.g. Hartmann 2009), which states that the accretion rate is $\dot{M} = 3\pi \Sigma_{\text{gas}} \nu_t$, with Σ_{gas} being the gas surface density and $\nu_t = \alpha k T_{\text{mid}} / \mu_g \Omega_K$ being the turbulent viscosity. The constant α is the ‘‘turbulent viscosity coefficient’’ which we take to be the standard value of $\alpha = 0.01$. This leads to the following powerlaw expression for the surface density of the gas:

$$\Sigma_{\text{gas}}(R) = C \dot{M} R^{-3/4} \quad \text{with} \quad C \equiv \frac{\mu \sqrt{GM_*}}{(3\pi)^{3/4} R_*^{3/4} \alpha k T_* f^{1/4}} \quad (16)$$

(valid for $\dot{M} \lesssim 10^{-8} M_\odot/\text{yr}$). Putting in our standard numbers we obtain: $\Sigma_{\text{gas}}(R) = 350 (R/\text{AU})^{-3/4} \text{ g/cm}^2$ for $\dot{M} = 10^{-8} M_\odot/\text{yr}$ (scaling linearly with \dot{M}). With the assumed opacities this validates the previous assumption that the disk is optically thick to the surface layer radiation for this accretion rate.

We can also estimate the pressure scale height $H_p(R)$, which (see Eq. 6) amounts to $H_p/R = 0.0167 (R/\text{AU})^{1/8}$ for our example model. Note that the ratio H_p/R (the disk opening angle) is nearly constant, at around 0.014. Unfortunately this result shows that the razor-thin disk assumption is not entirely justified, since $0.014 \times 0.5 \text{ AU} = 0.6 R_*$, meaning that at 0.5 AU the disk's pressure scale height is already half the star radius, and likely the surface height (where the disk becomes optically thin to stellar light incident at a small angle φ) substantially above that. So the model has to be refined, but as a rough estimate, it suffices.

Next we can calculate the opening angle of the shadow that the gas inner disk casts on the dust inner rim. For this we need the gas density, which follows from the application of Eq. (5) to the gas disk. We can then numerically integrate radially outward to the dust rim, assuming for simplicity now that the star is a point source, at various angles Θ with respect to the midplane ($\Theta = 0$ meaning through the midplane). This gives the radial column density of gas. Multiplying this with some guess of the gas opacity κ gives the optical depth for that κ , which is of course depending on ν . We can now plot, as a function of κ , at which Θ this optical depth drops below unity. This gives the half-opening-angle of the shadow cast by the gas disk for that particular value of κ . This plot is shown, for our model, in Fig. 14.

The angle Θ can be interpreted as follows. If the dust inner rim has a vertical optically thick surface height of about 0.2 AU at a distance of 1.5 AU (as we take from our example in Fig. 10) then a shadow of $\tan \Theta = 0.2/1.5 = 0.133$ would mean that the gas disk completely shadows the expected dust inner rim. This would mean that the dust rim model as it stands would not work. It will be cooler, and thus have a less high vertical extent, and it will emit little NIR flux. From Fig. 14 we get, however, that the shadow half-opening angle is at most $\Theta = 0.08$, for relatively high gas opacity as is present in some of the lines of water and TiO. However, for the opacity gap between 0.2 and 0.4 μm where, say, $\kappa \sim \text{few} \times 10^{-3} \text{ cm}^2/\text{g}$, the shadow is between $\Theta \simeq 0.02$ and $\Theta \simeq 0.05$. What we can conclude here is that the very midplane of the gas inner disk will likely cast some form of shadow on the inner dust rim. However, this shadow is likely not geometrically thick enough to cover the entire rim (MDCH04), and in particular in the opacity gap between 0.2 and 0.4 μm it is a relatively thin shadow. This situation is pictographically shown in Fig. 3. Moreover, the estimate in Fig. 14 is presumably overly pessimistic, because due to the finite stellar size, much of the radiation will simply move over the gas inner disk instead of through it. And finally, if the molecular abundances are substantially suppressed due to (photo-)dissociation, perhaps the shadow becomes weaker still.

5 Probing the inner dust-free disk with gas line observations

After some substantial theoretical modeling, let us return to observations, and focus in particular on what we can learn from high-spectral-resolution optical and near-infrared observations.

5.1 The search for molecules in the inner dust-free disk

Due to the absence of dust in the very inner disk regions, and the tentative theoretical expectation of substantial molecular content of the gas there, one may suspect that these regions are potent molecular line emitters. Interestingly, though, so far molecular line emission from these regions is only occasionally seen. In part this may be because of current observational limitations. But there is some evidence that there may be a true deficit of molecules in the dust-free inner disk.

Najita et al. (2007) recently reviewed the major results from high spectral resolution observations on YSO disk using large aperture telescopes, including a number of studies that impact the inner AU of disks. The high orbital velocities of the material in the inner disk as well as the high excitation temperatures of ro-

vibrational transitions of molecules such as CO and H₂O can be used to probe the dynamical and chemical compositions of these inner disks in a powerful way. CO fundamental lines are commonly observed in YSO disks and likely form in the surface layers of the disk over a large range of radii (from $\lesssim 0.1$ AU out to ~ 2 AU for solar mass young stars Najita et al., 2007). Interestingly, the CO overtone lines, which are collisionally populated by hot gas at >1000 K, are much more rare: only a few percent of T Tauri stars surveyed. In the rare cases where CO overtone lines are strong, often hot water bands are also seen (Carr, Tokunaga & Najita, 2004; Najita et al., 2009; Thi & Bik, 2005). CO overtone emission probably originates from the very inner regions (~ 0.05 AU to 0.3 AU for solar mass young stars Najita et al., 2007). Since R_{rim} for these stars is expected to lie roughly near 0.1 AU, the rarity of overtone emission seems to suggest that much of the molecular content is destroyed in the dust-free inner gas disk. However, it should be kept in mind that overtone emission requires not only a higher temperature, but also a higher column of CO than fundamental emission to be detectable. So it could equally well mean that most of the gas in this dust-free inner disk is cooler than expected, and that the total column of hot gas is too low for detectable overtone emission.

A recent advance in NIR interferometry is “spectro-interferometry”, in which the interferometric signal (visibility) can be measured as a function of wavelength. If the NIR flux of an object contains an interesting gas-phase line, then by determining the change in visibility over this line the differences in spatial scale of the emission of the gas line and the underlying continuum can be established. In some cases one can even retrieve information for different velocity components. This technique was pioneered for H- α observations in the visible for classical Be stars (Mourard et al., 1989), and was first applied to Br- γ emission measurements of YSOs by Malbet et al. (2007) for the wind-dominated Herbig-Be star MWC 297 and in the normal Herbig Ae star HD 104237 by Tatulli et al. (2007). The latter result was shocking: the Br- γ was not coming from the accretion flows as expected, but was arising from an extended region just inside the dust evaporation radius. Subsequent measurements on larger datasets (Kraus et al., 2008; Eisner et al., 2009) find a diversity of size scales for the Br- γ emission, from point-like to extended. The spatial extent can be both larger and smaller than that of the continuum. A comprehensive understanding has yet to emerge but may be related to the strength of the inner disk wind in Herbig Ae/Be stars. The distribution of Br- γ emission is possibly linked to the hot inner disk emission observed in the continuum discussed in §4, since in some cases they are co-spatial.

Br- γ is typically the strongest gas signal seen with NIR spectro-interferometry. For the rest the visibilities as a function of wavelength have so far been observed to be rather “continuum like”. Sometimes a hint of molecular emission from the hot inner disk is observed, such as the CO overtone band heads in the spectrum of RW Aur (Eisner et al., 2009) or the weak water feature tentatively found in the inner disk of Herbig Ae star MWC 480 (Eisner, 2007). But these signals, if they are real, are very weak. In fact, high resolution spectroscopic single-telescope K-band observations of some of these same sources (Najita et al., 2009) do not show any strong molecular lines, no CO overtone nor emission from water or any other molecules, though CO fundamental emission is detected for MWC 480 (Blake & Boogert, 2004). A comparison to the molecular line forest expected from Fig. 13 suggests that maybe these inner gaseous disks are not nearly as rich in molecules as we expected. In fact, as pointed out by Benisty et al. (in press)

even gas continuum opacities such as H^- opacity seem to be in conflict with the data. This poses the question: what is causing the smooth continuum emission from inside the dust rim? Currently this seems to be an unsolved question.

It is really a mystery why YSO disks do not show stronger emission from molecules in the dust-free inner disk, given that the molecular emission is regularly seen in the surface layers of the disk in the dusty regions of these disks (Carr & Najita, 2008; Mandell et al., 2008; Salyk et al., 2008; Bitner et al., 2008). But there does seem to be evidence for molecules right within the dust rim itself, where perhaps the dust may play a role in protecting these molecules from the photodissociating radiation. A nice example of such an observation is the work by Lahuis et al. (2006). They reported the detection of hot organic molecules in absorption against the infrared continuum with Spitzer-IRS in the object IRS 46. They argue that these absorption lines are observed because the line of sight toward the hot inner dust rim is partly blocked by the back side of this rim. If confirmed, this would show that molecules are at least present in the dusty rim itself. Interestingly, variability of these absorption lines is observed (Lahuis in prep), suggesting that the rim may cause variable levels of extinction for some reason. This suggests some link to the idea, suggested by Natta et al. (2001); Dullemond et al. (2003); Pontoppidan et al. (2007), that variability in the rim, as seen under a strong inclination, may in fact be the cause of UX Orionis-type short-timescale extinction events seen in some sources.

5.2 Probing the dynamics of the inner gas disk

Apart from looking for the presence of molecules, the study of molecular lines from the inner disk also allows us to study the dynamics of these inner regions. A particularly powerful technique is the emerging specialty of spectro-astrometry in the infrared, where an AO-corrected large-aperture telescope is used to measure centroid shifts as a function of spectral channel. Breakthrough results by Pontoppidan et al. (2008) show Keplerian motion in the fundamental CO band with evidence for strong departures of symmetry in some sources, demonstrating that even single telescopes can access information at the sub-milli-arcsecond level in some cases. Also spectro-astrometry can uncover evidence of binarity when emission lines do not trace continuum (Baines et al., 2006).

Another technique that has proved useful for probing the kinematic and spatial properties of the innermost gas disk is spectro-polarimetry. By measuring the polarization of the continuum along with the polarization of the $\text{H}\alpha$ emission line at multiple velocity channels, one can deduce the geometry and rotation properties of the innermost gas (within a few stellar radii) in YSOs (e.g., Vink et al., 2002, 2005). Vink et al. (2005) find evidence that the innermost gas in T Tauri and Herbig stars is oriented in a rotating disk aligned with the outer disk seen by other techniques (e.g., millimeter or scattered light) and that the Herbig Ae disks are significantly optically-thinner than the T Tauri ones. The potential for this technique has not yet been fully realized and we hope to see continued progress (e.g., see recent work of Harrington & Kuhn, 2007; Mottram et al., 2007).

6 Summary and outlook

In this review we have shown that the inner $\sim\text{AU}$ of protoplanetary disks is an area of rich physics. It is the region where dust is chemically processed and

evaporated. We have seen that the early naive picture of a definite “evaporation radius” separating the dusty outer disk from a dust-free inner disk is too simple. Complex interplay between multi-dimensional radiative transfer, dust chemistry and dust evaporation, together with insufficiently well understood gas opacities, yield a picture in which the transition from the dusty outer disk to the dust-free inner disk is far more gradual and subtle than previously thought. The complexity of the physics involved is so great, that even after almost a decade of research no definite model is in sight. And in this review we have not even had the chance to touch upon additional highly important and complex inner-disk phenomena such as magnetospheric accretion and episodic/unstable accretion. This means that the inner regions of protoplanetary disks are still a fertile ground for exciting research in the years to come, both observationally and theoretically.

We have already touched upon a number of issues that we consider not yet resolved. But it may be useful to give here a summary of these – and a number of not-yet-mentioned – issues:

- *Radiative transfer:* Does/can the rim cast a shadow over the disk (“self-shadowing”)? How do radiation pressure and possibly photophoresis affect the distribution of dust in the inner rim region? Is the rim solely responsible for the NIR bump, or are there other sources as well, and what is the nature of these sources? Can disk winds contribute to the NIR bump?
- *Dust composition:* What is the interplay between chemistry, condensation, evaporation, turbulent mixing and drift of dust grains in the dust inner rim? And consequently, what is the composition of the dust in the rim? Does the dust mineralogical processing in the rim affect planet formation and/or the composition of planets and planetary debris?
- *Gas inward of the ‘dust rim’:* What is the cause of the observed emission inside the dust rim? What is the dominant source of opacity in this region: Molecular lines, atomic lines, gas continuum or dust after all? Why are only few molecular lines from these very inner regions observed so far? Is the gas inward of the dust rim optically thin or thick? Can the gas “protect” the dust by its shadow, thus allowing dust to survive closer to the star? What the emission mechanism for the Br- γ line in Herbig’s and T Tauris? Why does the spatial extent of this feature show such diversity?
- *Dynamical behavior:* What is the (hydro)dynamic behavior of the rim? Is it stable? How does the internal heating near the midplane of the disk by active accretion affect the structure of the inner disk? How do we understand the reports of short-term variability of the inner disk in some sources (Sitko et al., 2008; Tuthill et al., 2002; Millan-Gabet et al., 2006)? Any relation to production of micro-jets (Devine et al., 2000)?

These are just a number of issues, among many more. With advances in optical and infrared interferometry, with techniques such as spectropolarimetry and spectroastrometry, in particular on ELTs, and with more focus on variability of all measured observables, and last but not least, with continued improvement of theoretical modeling, we believe that in the coming 10 years we will likely find the answers to many of the above questions.

We thank H-P. Gail, C. Dominik, H. Linz, R. van Boekel, U. Jorgensen, C. Helling, Th. Henning, M. Min., R. Millan-Gabet, J. Najita, Th. Preibisch,

N. Calvet, S. Krauss, J. Bouwman, L. Waters and A. Natta for many interesting and useful discussions and comments that have helped us a lot.

References

1. Adams FC, Shu FH. 1986. *ApJ* 308:836
2. Akeson RL, Boden AF, Monnier JD, Millan-Gabet R, Beichman C, et al. 2005. *ApJ* 635:1173
3. Akeson RL, Ciardi DR, van Belle GT, Creech-Eakman MJ, Lada EA. 2000. *ApJ* 543:313
4. Akeson RL, Walker CH, Wood K, Eisner JA, Scire E, et al. 2005. *ApJ* 622:440
5. Baines D, Oudmaijer RD, Porter JM, Pozzo M. 2006. *MNRAS* 367:737
6. Bell KR, Cassen P, Klahr HH, Henning T. 1997. *ApJ* 486:372
7. Bethell T, Bergin E. 2009. *Science* 326:1675
8. Bitner MA, Richter MJ, Lacy JH, Herczeg GJ, Greathouse TK, et al. 2008. *ApJ* 688:1326
9. Bjorkman JE, Wood K. 2001. *ApJ* 554:615
10. Blake GA, Boogert ACA. 2004. *ApJ* 606:L73
11. Blum J, Wurm G. 2008. *ARAA* 46:21
12. Bockelée-Morvan D, Gautier D, Hersant F, Huré JM, Robert F. 2002. *A&A* 384:1107
13. Boekel RV, Dullemond CP, Dominik C. 2005. *A&A* 441:563
14. Boekel RV, Min M, Leinert C, Waters LBFM, Richichi A, et al. 2004. *Nature* 432:479
15. Bouvier J, Alencar SHP, Harries TJ, Johns-Krull CM, Romanova MM. 2007. *Protostars and Planets V* :479
16. Bouwman J, de Koter A, van den Ancker ME, Waters LBFM. 2000. *A&A* 360:213
17. Calvet N, Magris GC, Patino A, D'Alessio P. 1992. *Revista Mexicana de Astronomia y Astrofisica* 24:27
18. Calvet N, Patino A, Magris GC, D'Alessio P. 1991. *ApJ* 380:617
19. Carr JS, Najita JR. 2008. *Science* 319:1504
20. Carr JS, Tokunaga AT, Najita J. 2004. *ApJ* 603:213
21. Cesaroni R, Galli D, Lodato G, Walmsley CM, Zhang Q. 2007. *Protostars and Planets V* :197
22. Chiang EI, Goldreich P. 1997. *ApJ* 490:368
23. Cohen M, Kuhl LV. 1979. *ApJS* 41:743
24. Colavita M, Akeson R, Wizinowich P, Shao M, Acton S, et al. 2003. *ApJL* 592:L83
25. Corder S, Eisner J, Sargent A. 2005. *ApJL* 622:L133
26. D'Alessio P, Calvet N, Hartmann L, Muzerolle J, Sitko M. 2004. *Star Formation at High Angular Resolution* 221:403
27. D'Alessio P, Canto J, Calvet N, Lizano S. 1998. *ApJ* 500:411
28. Danchi WC, Tuthill PG, Monnier JD. 2001. *ApJ* 562:440

29. Devine D, Grady CA, Kimble RA, Woodgate B, Bruhweiler FC, et al. 2000. *ApJL* 542:L115
30. Dullemond CP, Ancker MEVD, Acke B, Boekel RV. 2003. *ApJ* 594:L47
31. Dullemond CP, Dominik C. 2004. *A&A* 417:159
32. Dullemond CP, Dominik C, Natta A. 2001. *ApJ* 560:957
33. Eisner JA. 2007. *Nature* 447:562
34. Eisner JA, Chiang EI, Lane BF, Akeson RL. 2007. *ApJ* 657:347
35. Eisner JA, Graham JR, Akeson RL, Najita J. 2009. *ApJ* 692:309
36. Eisner JA, Hillenbrand LA, White RJ, Akeson RL, Sargent AI. 2005. *ApJ* 623:952
37. Eisner JA, Lane BF, Akeson RL, Hillenbrand LA, Sargent AI. 2003. *ApJ* 588:360
38. Eisner JA, Lane BF, Akeson RL, Hillenbrand LA, Sargent AI. 2003. *ApJ* 588:360
39. Eisner JA, Lane BF, Hillenbrand LA, Akeson RL, Sargent AI. 2004. *ApJ* 613:1049
40. Eisner JA, Lane BF, Hillenbrand LA, Akeson RL, Sargent AI. 2004. *ApJ* 613:1049
41. Ekberg U, Eriksson K, Gustafsson B. 1986. *A&A* 167:304
42. Friedjung M. 1985. *A&A* 146:366
43. Gail HP. 1998. *A&A* 332:1099
44. Gail HP. 2001. *A&A* 378:192
45. Gail HP. 2002. *A&A* 390:253
46. Gail HP. 2004. *A&A* 413:571
47. Glassgold AE, Meijerink R, Najita JR. 2009. *ApJ* 701:142
48. Glassgold AE, Najita J, Igea J. 2004. *ApJ* 615:972
49. Haisch KE, Lada EA, Lada CJ. 2001. *ApJ* 553:L153
50. Harrington DM, Kuhn JR. 2007. *ApJL* 667:L89
51. Hartmann L. 2009. *Accretion Processes in Star Formation*. Cambridge, UK: Cambridge University Press, 2009
52. Hartmann L, Kenyon SJ. 1985. *ApJ* 299:462
53. Hartmann L, Kenyon SJ, Calvet N. 1993. *ApJ* 407:219
54. Helling C, Lucas W. 2009. *MNRAS* :1102
55. Henning T, Meeus G. 2009. *arXiv astro-ph*
56. Hillenbrand LA, Strom SE, Vrba FJ, Keene J. 1992. *ApJ* 397:613
57. Isella A, Natta A. 2005. *A&A* 438:899
58. Isella A, Tatulli E, Natta A, Testi L. 2008. *A&A* 483:L13
59. Isella A, Tatulli E, Natta A, Testi L. 2008. *A&A* 483:L13
60. Isella A, Testi L, Natta A. 2006. *A&A* 451:951
61. Juhász A, Prusti T, Ábrahám P, Dullemond CP. 2007. *MNRAS* 374:1242
62. Kama M, Min M, Dominik C. 2009. *A&A* 506:1199
63. Kenyon SJ, Hartmann L. 1987. *Astrophysical Journal* 323:714
64. Kraus S, Hofmann KH, Benisty M, Berger JP, Chesneau O, et al. 2008. *A&A* 489:1157

65. Kraus S, Preibisch T, Ohnaka K. 2008. *ApJ* 676:490
66. Lahuis F, Dishoeck EV, Boogert ACA, Pontoppidan KM, Blake GA, et al. 2006. *ApJ* 636:L145
67. Lucy LB. 1999. *A&A* 344:282
68. Malbet F, Benisty M, de Wit WJ, Kraus S, Meilland A, et al. 2007. *A&A* 464:43
69. Malbet F, Berger JP, Colavita MM, Koresko CD, Beichman C, et al. 1998. *ApJL* 507:L149
70. Malfait K, Bogaert E, Waelkens C. 1998. *A&A* 331:211
71. Mandell AM, Mumma MJ, Blake GA, Bonev BP, Villanueva GL, Salyk C. 2008. *ApJL* 681:L25
72. McCaughrean MJ, O'Dell C. 1996. *AJ* 111:1977
73. Meeus G, Waters LBFM, Bouwman J, Ancker MEVD, Waelkens C, Malfait K. 2001. *A&A* 365:476
74. Men'shchikov AB, Henning T. 1997. *A&A* 318:879
75. Mihalas D, Mihalas BW. 1984. *Foundations of radiation hydrodynamics*. New York
76. Millan-Gabet R, Malbet F, Akeson R, Leinert C, Monnier J, Waters R. 2007. In *Protostars and Planets V*, eds. B Reipurth, D Jewitt, K Keil
77. Millan-Gabet R, Monnier JD, Berger JP, Traub WA, Schloerb FP, et al. 2006. *ApJL* 645:L77
78. Millan-Gabet R, Schloerb FP, Traub WA. 2001. *ApJ* 546:358
79. Millan-Gabet R, Schloerb FP, Traub WA, Malbet F, Berger JP, Bregman JD. 1999. *ApJL* 513:L131
80. Min M, Dullemond CP, Dominik C, Koter AD, Hovenier JW. 2009. *A&A* 497:155
81. Miroshnichenko A, Ivezić Ž, Vinković D, Elitzur M. 1999. *ApJL* 520:L115
82. Monnier JD. 2007. *New Astronomy Review* 51:604
83. Monnier JD, Berger JP, Millan-Gabet R, Traub WA, Schloerb FP, et al. 2006. *ApJ* 647:444
84. Monnier JD, Millan-Gabet R. 2002. *ApJ* 579:694
85. Monnier JD, Millan-Gabet R. 2002. *ApJ* 579:694
86. Monnier JD, Millan-Gabet R, Billmeier R, Akeson RL, Wallace D, et al. 2005. *ApJ* 624:832
87. Monnier JD, Millan-Gabet R, Billmeier R, Akeson RL, Wallace D, et al. 2005. *ApJ* 624:832
88. Monnier JD, Zhao M, Pedretti E, Thureau N, Ireland M, et al. 2007. *Science* 317:342
89. Mottram JC, Vink JS, Oudmaijer RD, Patel M. 2007. *MNRAS* 377:1363
90. Mourard D, Bosc I, Labeyrie A, Koechlin L, Saha S. 1989. *Nature* 342:520
91. Muzerolle J, Calvet N, Hartmann L, D'Alessio P. 2003. *ApJL* 597:L149
92. Muzerolle J, Calvet N, Hartmann L, D'Alessio P. 2003. *ApJ* 597:L149
93. Muzerolle J, D'Alessio P, Calvet N, Hartmann L. 2004. *ApJ* 617:406

94. Muzerolle J, Flaherty K, Balog Z, Furlan E, Smith PS, et al. 2009. *The Astrophysical Journal Letters* 704:L15
95. Najita JR, Carr JS, Glassgold AE, Valenti JA. 2007. In *Protostars and Planets V*, eds. B Reipurth, D Jewitt, K Keil
96. Najita JR, Doppmann GW, Carr JS, Graham JR, Eisner JA. 2009. *ApJ* 691:738
97. Natta A, Prusti T, Neri R, Wooden D, Grinin VP, Mannings V. 2001. *A&A* 371:186
98. Nomura H. 2002. *ApJ* 567:587
99. Pezzuto S, Strafella F, Lorenzetti D. 1997. *ApJ* 485:290
100. Pinte C, Harries TJ, Min M, Watson AM, Dullemond CP, et al. 2009. *A&A* 498:967
101. Pollack JB, Hollenbach D, Beckwith SVW, Simonelli DP, Roush T, Fong W. 1994. *ApJ* 421:615
102. Pontoppidan KM, Blake GA, van Dishoeck EF, Smette A, Ireland MJ, Brown J. 2008. *ApJ* 684:1323
103. Pontoppidan KM, Dullemond CP, Blake GA, Boogert ACA, Dishoeck EV, et al. 2007. *ApJ* 656:980
104. Rybicki GB, Lightman A. 1979. *John Wiley & Sons*
105. Salyk C, Pontoppidan KM, Blake GA, Lahuis F, van Dishoeck EF, Evans II NJ. 2008. *ApJL* 676:L49
106. Shang H, Li ZY, Hirano N. 2007. *Protostars and Planets V* :261
107. Sitko ML, Carpenter WJ, Kimes RL, Wilde JL, Lynch DK, et al. 2008. *ApJ* 678:1070
108. Tannirkulam A, Harries TJ, Monnier JD. 2007. *ApJ* 661:374
109. Tannirkulam A, Harries TJ, Monnier JD. 2007. *ApJ* 661:374
110. Tannirkulam A, Monnier JD, Harries TJ, Millan-Gabet R, Zhu Z, et al. 2008. *ApJ* 689:513
111. Tannirkulam A, Monnier JD, Harries TJ, Millan-Gabet R, Zhu Z, et al. 2008a. *ApJ* 689:513
112. Tannirkulam A, Monnier JD, Millan-Gabet R, Harries TJ, Pedretti E, et al. 2008b. *ApJ* 677:L51
113. Tatulli E, Isella A, Natta A, Testi L, Marconi A, et al. 2007. *A&A* 464:55
114. Terquem CEJMLJ. 2008. *ApJ* 689:532
115. Thi WF, Bik A. 2005. *A&A* 438:557
116. Tuthill PG, Monnier JD, Danchi WC. 2001. *Nature* 409:1012
117. Tuthill PG, Monnier JD, Danchi WC, Hale DDS, Townes CH. 2002. *ApJ* 577:826
118. Tuthill PG, Monnier JD, Danchi WC, Wishnow EH, Haniff CA. 2000. *Proc.Astr.Soc.Pacific* 112:555
119. Vink JS, Drew JE, Harries TJ, Oudmaijer RD. 2002. *MNRAS* 337:356
120. Vink JS, Drew JE, Harries TJ, Oudmaijer RD, Unruh Y. 2005. *MNRAS* 359:1049
121. Vinković D. 2006. *ApJ* 651:906

122. Vinković D, Ivezić Ž, Jurkić T, Elitzur M. 2006. *ApJ* 636:348
123. Vinković D, Ivezić Ž, Jurkić T, Elitzur M. 2006. *ApJ* 636:348
124. Vinković D, Ivezić Ž, Miroshnichenko AS, Elitzur M. 2003. *MNRAS* 346:1151
125. Vinković D, Jurkić T. 2007. *ApJ* 658:462
126. Watson AM, Stapelfeldt KR, Wood K, Ménard F. 2007. *Protostars and Planets V* :523
127. Wisniewski JP, Clampin M, Grady CA, Ardila DR, Ford HC, et al. 2008. *ApJ* 682:548
128. Wood K. 2008. *New Astronomy Reviews* 52:145
129. Zolensky ME, Zega TJ, Yano H, Wirick S, Westphal AJ, et al. 2006. *Science* 314:1735

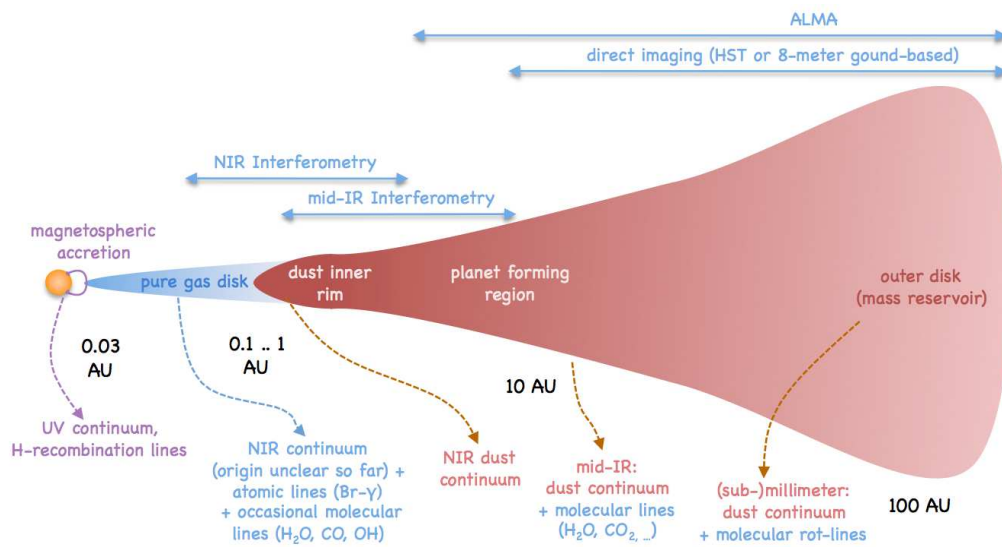


Figure 1: Pictogram of the structure and spatial scales of a protoplanetary disk. Note that the radial scale on the x-axis is not linear. Above the pictogram it is shown which techniques can spatially resolve which scales. Below it is shown which kind of emission arises from which parts of the disk.

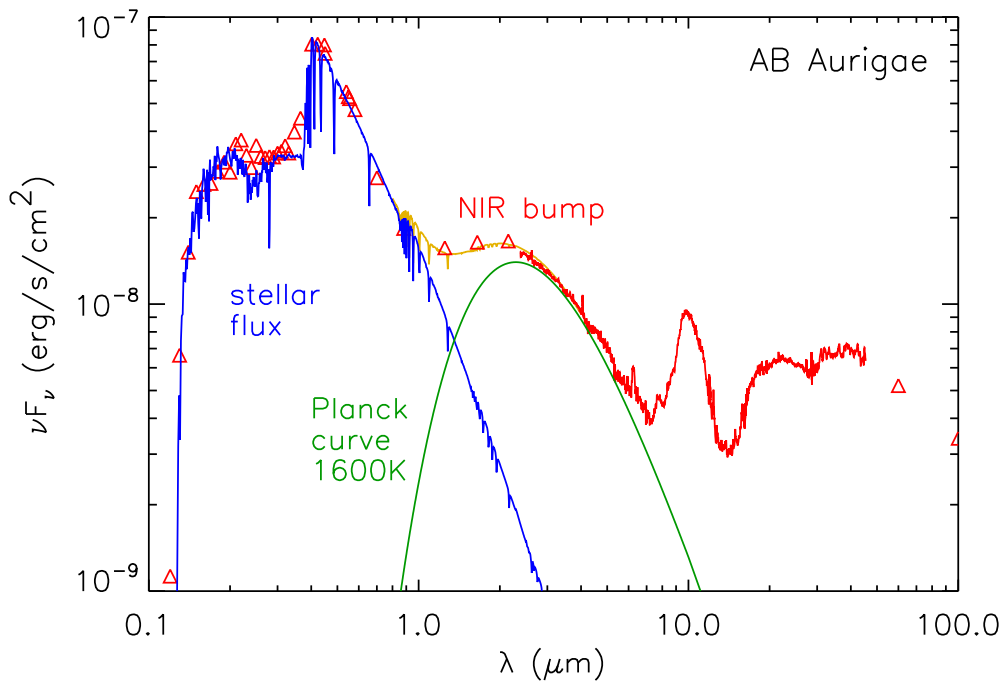


Figure 2: The spectral energy distribution of the Herbig Ae star AB Aurigae. Red is the measured emission. Blue is the stellar spectrum predicted with a Kurucz stellar atmosphere model. The excess of flux above the atmosphere (the “infrared excess”) is the thermal emission from the dust in the disk. The emission in the near infrared clearly has a bump-like structure, and is often called the “near infrared bump”. In green a Planck curve at a temperature of 1600 K is overplotted. The golden curve is the sum of the Planck curve and the stellar atmosphere.

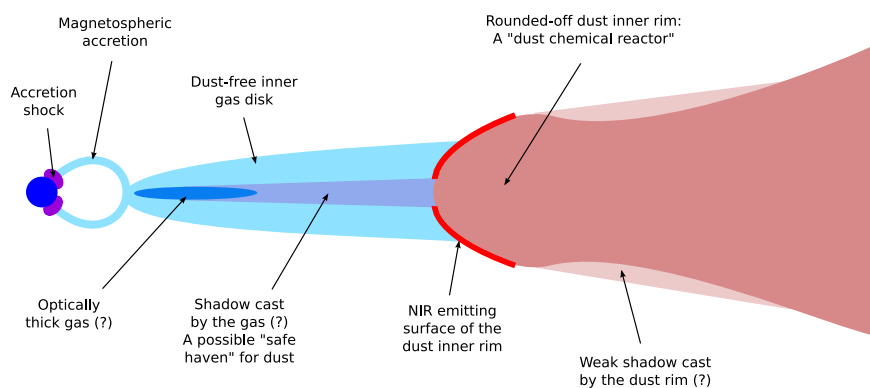


Figure 3: Pictographic representation of the inner disk region out to a few AU. One sees the magnetospheric accretion depicted near the star, the dust-free gas disk in the middle and the dust rim on the right.

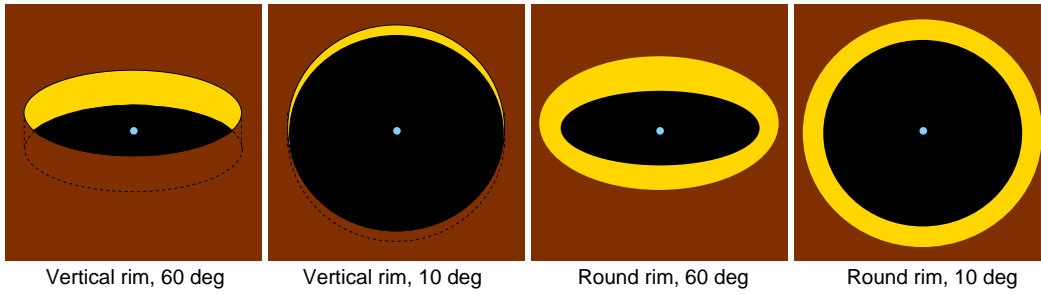


Figure 4: Pictographic representation of how an inner rim is viewed. The left two panels show a simple vertical rim model while the right two panels show a rounded-off rim. In both cases the left panel shows the rim at an inclination of about 60 degrees while the right panels shows it at near face-on inclination (10 degrees). The yellow color represents the emission from the hot dust that is in direct sight of the star and thus heated to high temperatures. Brown is the cooler dust behind the rim.

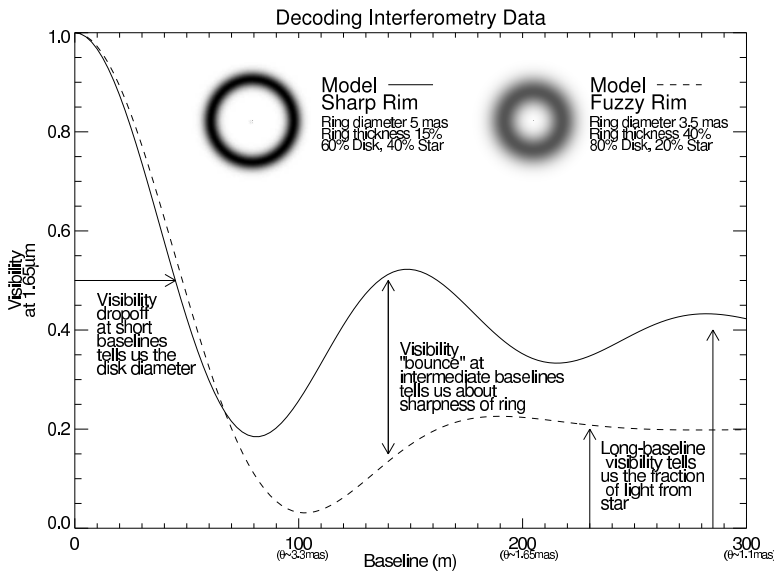


Figure 5: *caption for box inset:*

Single-baseline infrared interferometers have revolutionized our understanding of the inner disk of young stellar objects by measuring the size scale and morphology of the dust and gas at the inner edge within an AU of the central star. In this figure, we present a primer on how to decode interferometer data as typically presented in observational papers.

The interferometer measures the object's "Visibility" as a function of the telescopes separation ("Baseline"), with longer baselines probing finer angular scales. Here we show two simple examples of inner disks, a "Sharp Rim" model and a "Fuzzy Rim" Model – the intensity images are shown are included too. Using arrows and labels, we show how measurements at different baselines can be used to directly constrain the (i) size of the disk, (ii) the sharpness of the rim, and (iii) the fraction of light coming from the star and disk. By combining multi-wavelength measurements from multiple interferometers such as VLTI, Keck, and CHARA we can now span a wide range of spatial scales necessary to unmask the true nature and morphology of the inner regions of YSO disks. New instruments are being developed now to allow true imaging within the next few years.

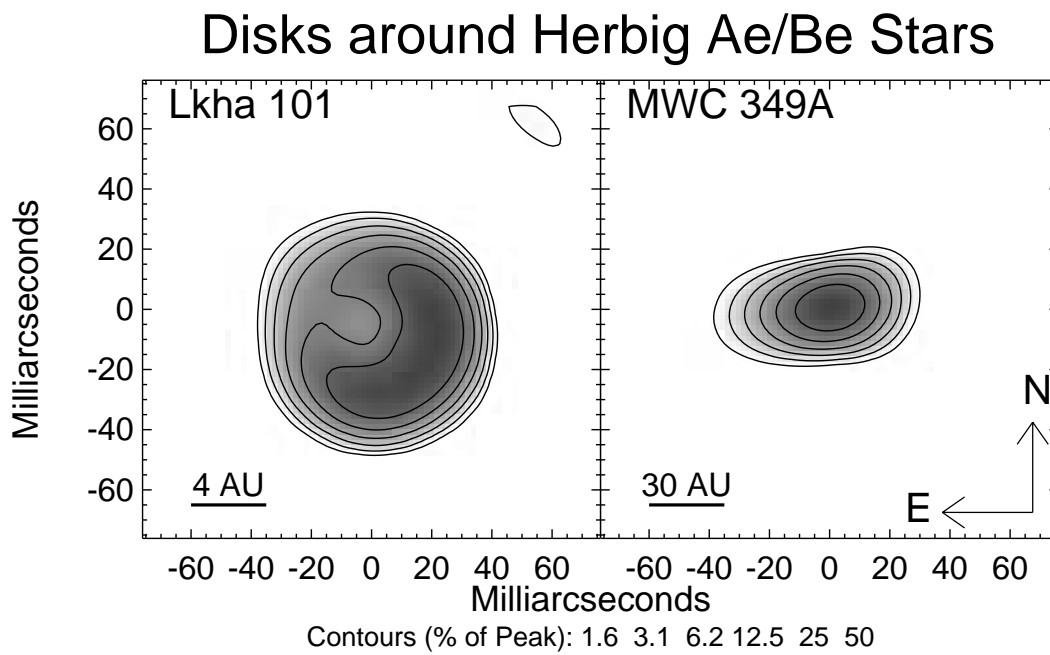


Figure 6: These K-band images from Keck aperture masking showed the inner disks of the Herbig Be stars LkH α 101 (Tuthill, Monnier & Danchi, 2001) and MWC 349 (Danchi, Tuthill & Monnier, 2001). The dust-free inner cavity in LkH α 101 was much larger than expected.

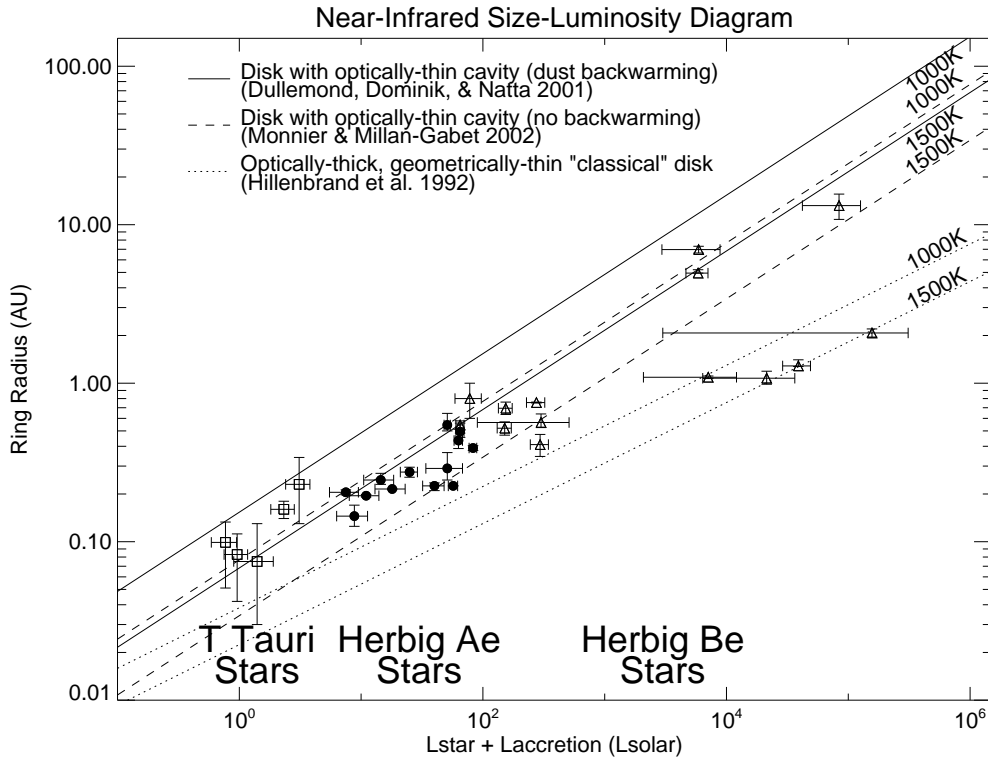


Figure 7: The size-luminosity diagram obtained from NIR interferometric measurements of T Tauri and Herbig Ae stars (adapted from figure presented in Millan-Gabet et al., 2007). The observed near-infrared sizes can be compared against different disk models, including disks with optically-thin cavities and those that are optically-thick but geometrically thin. The most realistic disk models that include backwarming suggest dust evaporation temperatures are between 1500–2000K.

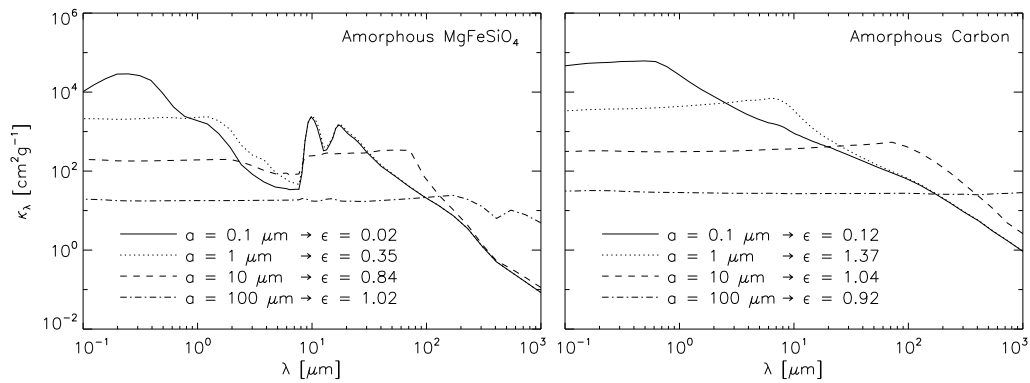


Figure 8: Absorption opacity per gram of dust for different dust grain sizes, assuming spherical compact grains. Left: amorphous olivine. Right: amorphous carbon. The ϵ values according to Eq. (10) for a stellar blackbody temperature of $T_* = 10000\text{K}$ and a dust temperature of $T_{\text{dust}} = 1500\text{K}$ are also given in the figure. Note that in reality in the inner rim the dust is presumably crystalline, but it is unclear what exact composition the dust will have then. For a review of astronomical dust and its opacities, see e.g. Henning & Meeus (2009) and Henning (THIS ISSUE OF ARAA).

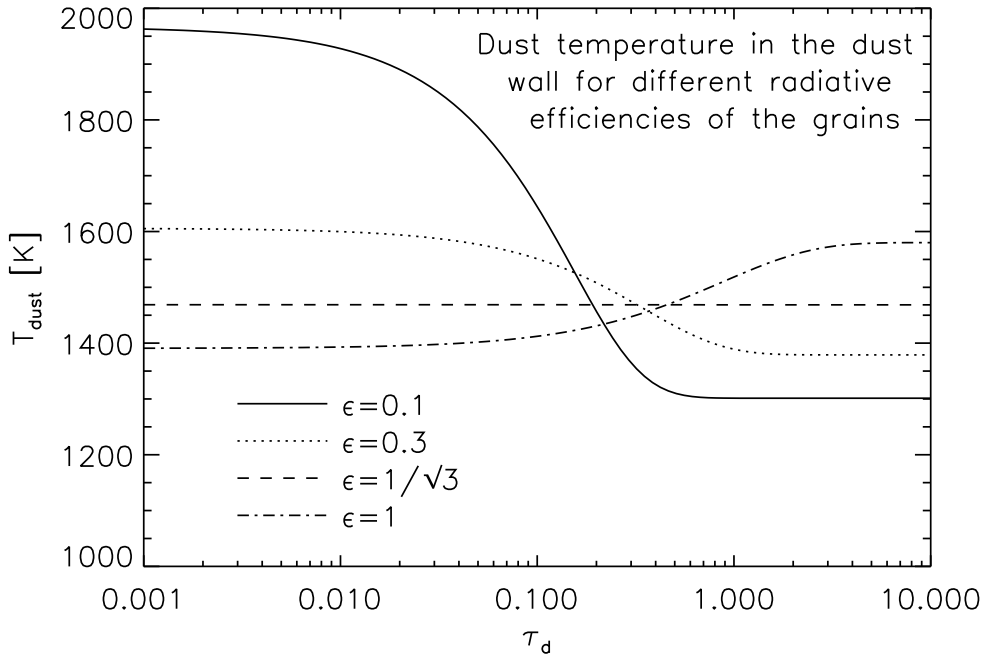


Figure 9: The run of temperature with depth into the dust rim of our AB Aurigae example case, where τ_d is the optical depth in the NIR. The inner boundary of this model lies at 0.5 AU from the star. The stellar radiation enters the rim perpendicularly to the rim wall, i.e. $\mu = 1$ in the equations in the text. The solution is shown for four different kinds of dust, i.e. four efficiency factors ϵ . The case of $\epsilon = 1$ corresponds typically to large dust grains ($a \gg 3\mu\text{m}$) while smaller dust grains lead to smaller ϵ . Note that the entire solution shown here corresponds only to a very thin layer at the inside of the dust wall.

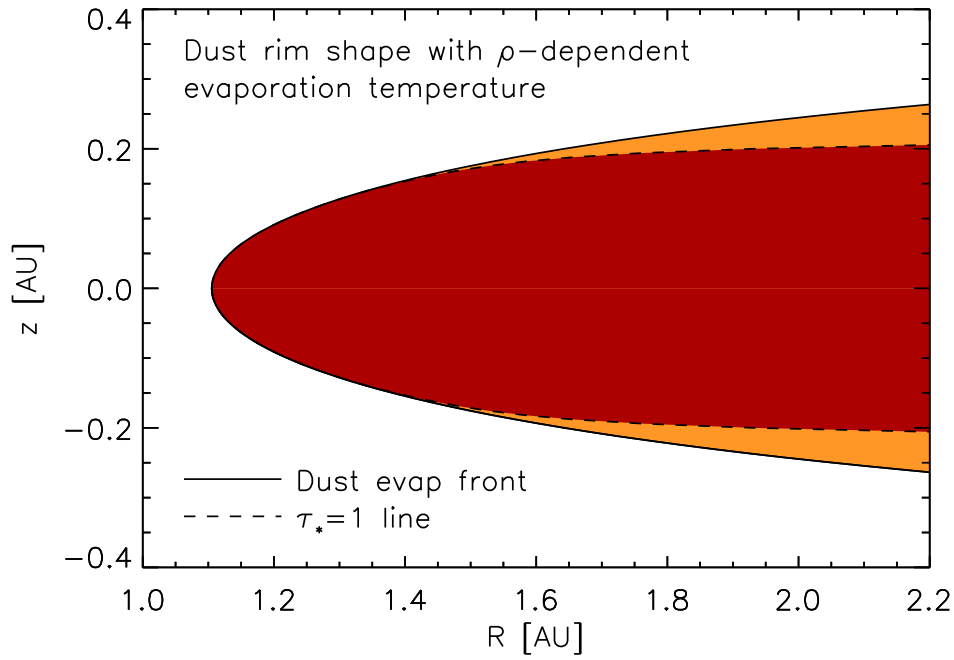


Figure 10: The rounded-off rim model of IN05 computed using Eq. (13), which is a simplified version of the IN05 model. Parameters are $R_* = 2.4 R_\odot$, $M_* = 2.4 M_\odot$, $T_* = 10000$, $\epsilon = 0.1$, $H_{p,\text{rim}} = 0.044$ AU, $\Sigma_{\text{gas}} = 100$ g/cm² and $\epsilon = 0.1$. The brown region is the region that contains dust. The dark brown sub-region is the region that is more than $\tau_* = 1$ shielded from the stellar radiation field, where τ_* is defined as the radially outward optical depth at the average stellar wavelength. The midplane gas density at $\tau_* = 1$ in this model is $\rho_g = 6 \times 10^{-11}$ g/cm³.

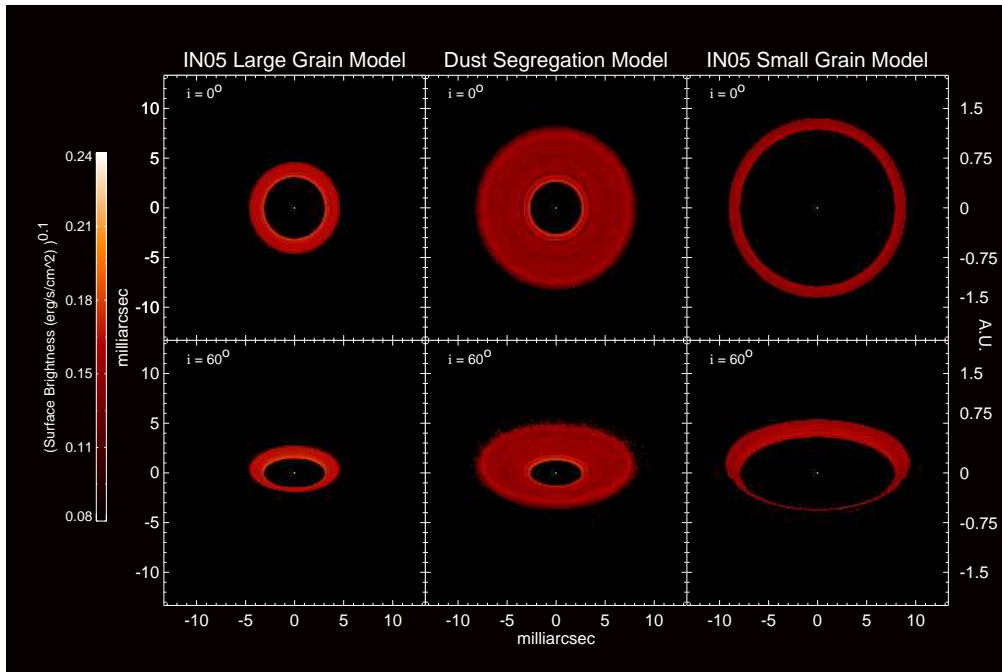


Figure 11: Middle column: Model images of the first 2-D self-consistent rounded-off rim model (Tannirkulam, Harries & Monnier, 2007). Left and right columns: the IN05 model for small (left) and large (right) grains. The Tannirkulam model includes, in addition to the dust evaporation physics, also a simple treatment of dust growth and sedimentation.

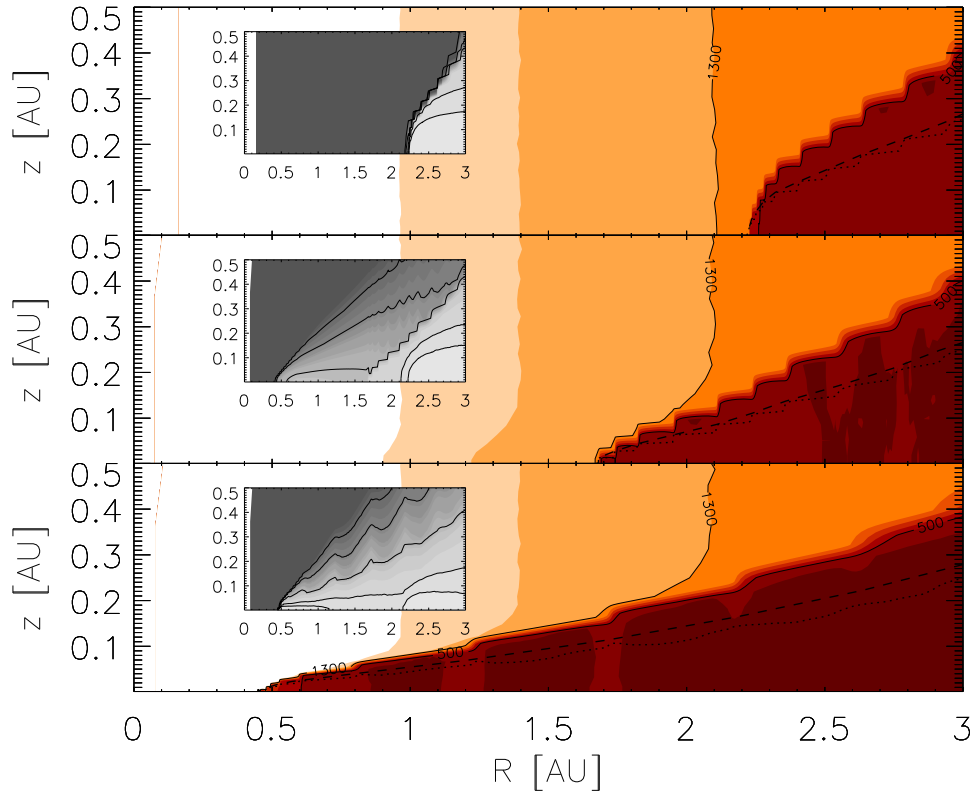


Figure 12: Model result of Kama, Min & Dominik (2009) for the temperature structure (red color map) and density structure (grey scale insets) of the inner rim of a disk around a star with $M_* = 2.4 M_\odot$, $R_* = 2.4 R_\odot$, $T_* = 10000$ K, for a gas surface density of $\Sigma_g = 100$ g/cm². The temperature color contours are in steps of 200 K. Density contours are a factor 2.7, 10, 10^4 , 10^7 and 10^{10} below the maximum. Upper panel: only small $0.1 \mu\text{m}$ olivine grains, yielding a sharp rim. Middle panel: 1% of small olivines replaced by $10 \mu\text{m}$ olivine grains, rest stays small. Lower panel: Like middle panel but now replacing 10%.

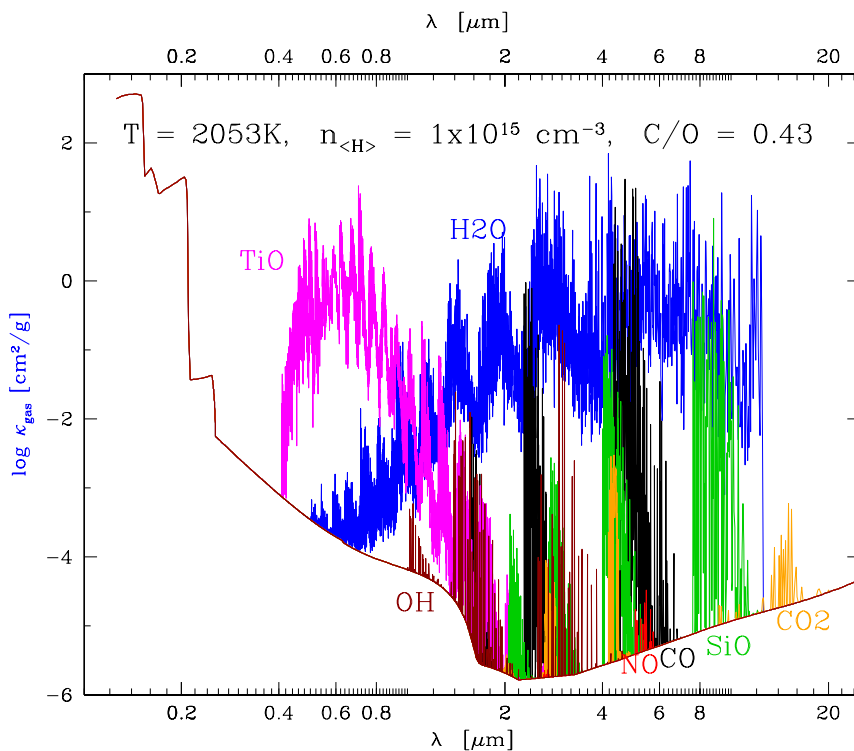


Figure 13: An example of opacities of the gas at conditions typical for the inner dust-free region of the disk. The abundances of the various sources of opacity (TiO, H₂O being the dominant line absorption agents) are calculated using equilibrium chemistry at the temperature of 2053 K. No photodissociation of the molecules is included which might substantially reduce the strength of the molecular line contribution to the opacity. From Ch. Helling priv comm., used with permission (see Helling & Lucas, 2009, for details on the computations).

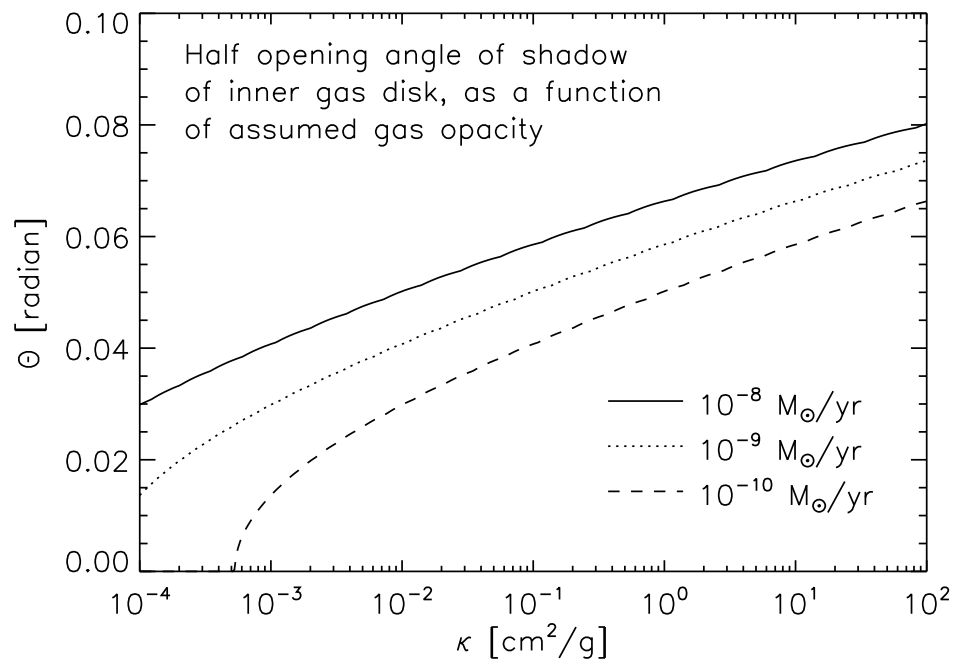


Figure 14: The half-opening-angle of the shadow cast by the gaseous dust-free inner disk as a function of gas opacity κ , for our standard example star and for three different accretion rates. The inner radius was assumed to be at 0.03 AU and the outer radius at 0.5 AU. See text for details.